Synthesis, Radiosynthesis, and Biological Evaluation of Carbon-11 and Iodine-123 Labeled 2β-Carbomethoxy-3β-[4′-((*Z*)-2-haloethenyl)phenyl]tropanes: Candidate Radioligands for in Vivo Imaging of the Serotonin Transporter

Christophe Plisson, Jonathan McConathy, Laurent Martarello, Eugene. J. Malveaux, Vernon M. Camp, Larry Williams, John R. Votaw, and Mark M. Goodman*

Department of Radiology, Emory University, Atlanta, Georgia 30320

Received August 8, 2003

2β-Carbomethoxy-3β-[4′-((*Z*)-2-iodoethenyl)phenyl]tropane (ZIET) and 2β-carbomethoxy-3β-[4′-((*Z*)-2-bromoethenyl)phenyl]tropane (ZBrET) were synthesized as well as their nortropane congeners ZIENT and ZBrENT. Binding affinities of these compounds were determined in cells transfected to express human SERT, DAT, and NET using [^{3}H]citalopram, [^{125}I]RTI-55, and [^{3}H]nisoxetine, respectively. Both ZIET and ZBrET displayed high affinity for the SERT (K_i = 0.11 and 0.08 nM, respectively).The affinities of ZIET and ZBrET for the DAT were 200 and 38-fold lower, respectively, than for the SERT. [^{11}C]ZIET and [^{11}C]ZBrET were prepared by alkylation of their corresponding nortropanes with [^{11}C]methyl iodide in approximately 30% radiochemical yield (decay-corrected to end of bombardment, EOB). High specific activity [^{123}I]ZIET was synthesized in 33% radiochemical yield (decay-corrected) by treating the 2β-carbomethoxy-3β-[4′-((*Z*)-2-trimethylstannylethenyl)phenyl]tropane (**3**) with no carrier-added sodium [^{123}I]iodide and hydrogen peroxide in ethanolic HCl. Biodistribution studies in rats indicated that [^{123}I]ZIET enters the brain readily and accumulates in SERT-rich regions. Blocking studies performed in rats demonstrated that [^{123}I]ZIET was selective and specific for SERT-rich regions (e.g. thalamus, brainstem, and striatum). MicroPET brain imaging studies in monkeys demonstrated that [^{11}C]ZIET and [^{11}C]ZBrET uptakes were selectivity localized in the putamen, midbrain, caudate, thalamus, pons, and medulla. Radioactivity in the regions of high SERT density of monkey brain was displaceable with citalopram except in the putamen and caudate. Radioactivity uptake in these DAT-rich regions was significantly displaceable either by preadministration of citalopram followed by injection of RTI-113 (or vice-versa) or by administration of a mixture of DAT and SERT ligands. In conclusion, the high yield, high specific activity, one-step radiolabeling method, high selectivity and favorable kinetics, and the good results obtained with [^{123}I]ZIET in rats support the candidacy of [^{11}C]ZIET for in vivo visualization and quantification of brain SERT.

Introduction

The serotonin transporter (SERT) is a protein residing on the presynaptic serotonergic neuron that regulates the serotonin concentration by removing serotonin from the extracellular space back to the presynaptic neuron. Because of its localization, the SERT is a specific marker for serotonergic neurons.[1−4] Serotonergic neurons originate primarily from neuronal cell bodies of the medial and dorsal raphe in the brainstem and innervate discrete areas that include the hypothalamus, thalamus, striatum, and cerebral cortex.[5−7] Therefore, in vivo imaging of the SERT in humans with PET or SPECT would permit the study of the density and integrity of serotonin neurons and help to understand how alterations in SERT levels are related to numerous neuropsychiatric disorders such as depression,[8] Alzheimer's disease,[9] Parkinson's disease[10,11] and the neurotoxic effects of illicit drugs (e.g. MDMA).[12]

A number of useful radioligands for both PET and SPECT have been developed and evaluated for imaging the SERT in the central nervous system (CNS).[13,6,14] Most of them appeared to be unsuitable for imaging due to high lipophilicity and/or high nonspecific binding and/or inappropriate in vivo kinetics.[15] The first imaging agent successfully employed in humans for studying the SERT was the cocaine analogue [^{123}I] 2β-carbomethoxy-3β-(4′-iodophenyl)tropane ([^{123}I]β-CIT) (Scheme 1). However, because of its lack of selectivity for the SERT versus DAT (dopamine transporter), the evaluation of the SERT sites is limited to areas outside the DAT-rich striatum or requires preblocking of the DAT sites.[16] The most widely used PET imaging agent of the SERT currently available is a pyrroloisoquinoline derivative, (+)-[^{11}C]McN-5652.[17−19] This radioligand, which has been used in human studies of SERT density, has significant limitations such as modest signal to back-

Scheme 1

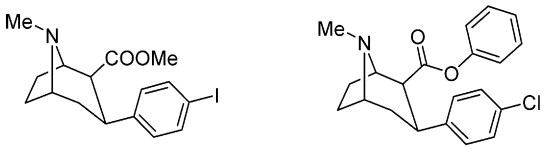

β-CIT RTI-113

* Corresponding author:Mark M. Goodman, Ph. D. Emory University, Department of Radiology 1364 Clifton Road, NE, Atlanta, GA 30322; Phone: (404) 727-9366; Fax: (404) 727-3488; e-mail: mgoodma@emory.edu.

10.1021/jm030384e CCC: $27.50
Published on Web 02/03/2004

Table 1. In Vitro Evaluation of Various Ligands in Competition Assays with Human Monoamine Transporters[a]

compound	K_i for hSERT	K_i for hDAT	K_i for hNET	hSERT/hDAT ratio
ZIENT[b]	0.05	3.5	24	70
ZIET	0.11 ± 0.006	22 ± 9	450 ± 24	200
ZIENT	0.04 ± 0.01	15 ± 1.4[c]	N.D.	375
ZBrET	0.08 ± 0.01	3.1 ± 0.3	111 ± 12	38
ZBrENT	0.04 ± 0.007	3.9 ± 0.6	2.5	97
8	0.08 ± 0.006	5.6 ± 3	5.6	70
9	1.35 ± 0.10	6.73 ± 0.63	161 ± 17	5
β-CIT[d]	4.2	1.3	36	0.3
nor-β-CIT[d]	0.36	0.69	7.5	2
RTI-113[e]	390 ± 34.26	5.25 ± 0.76	242.29 ± 29.78	0.013
R,S-citalopram[f]	1.6 ± 0.1	16 540 ± 3795	6190 ± 818	10337
reboxetine[g]	129 ± 13	>10 000	1.1 ± 0.2	

[a] In vitro evaluation of candidate SERT ligands in competition assays using cells transfected with human monoamine transporters. All K_i values are reported with nanomolar (nM) units. At least three separate K_i determinations were performed for each compound unless otherwise indicated. The data are expressed as the geometric mean ± standard deviation. The hSERT/hDAT ratios reflect the affinity ($1/K_i$) for hSERT divided by the affinity for hDAT. [b] Previous values from competition assays performed using cells transfected with hSERT, hDAT, or hNET.[28] hDAT competition assays were performed using [^{3}H]WIN 35,428 as the radiotracer, while in the current study [^{125}I]RTI-55 was used. [c] Average value of two separate K_i determinations. [d] Literature values (IC_{50}) from competition assays performed with rat brain homogenates using [^{3}H]paroxetine for SERT, [^{3}H]WIN 35,428 for DAT, and [^{3}H]nisoxetine for NET.[35] [e] Literature values (K_i) from competition assays performed with rat brain homogenates using [^{3}H]paroxetine for SERT, [^{3}H]WIN 35,428 for DAT, and [^{3}H]nisoxetine for NET.[36] [f] Literature values (K_i) from competition assays performed using cells transfected with hSERT, hDAT or hNET using [^{3}H]citalopram, [^{125}I]RTI-55, and [^{3}H]nisoxetine.[37] [g] Literature values (K_i) from competition assays performed with rat brain membranes labeled by [^{3}H]paroxetine for SERT, [^{3}H]WIN 35,428 for DAT, and [^{3}H]nisoxetine for NET.[38]

ground due to high nonspecific binding. More recently a new class of radiotracers from the diaryl sulfide class has been introduced such as [^{123}I]ADAM,[20] [^{11}C]-DASB,[15,21,22] [^{11}C]AFM,[15,23] [^{11}C]EADAM,[24] and [^{18}F]-ACF.[25] Compounds from this class have been labeled with ^{123}I for SPECT and ^{11}C or ^{18}F for PET. They demonstrated high in vitro affinity and selectivity to the SERT with low affinity for the DAT and NET (norepinephrine transporter). The carbon-11 series of diaryl sulfides showed higher in vitro selectivity but higher lipophilicity and lower affinity to SERT than the tropanes reported in this article. Evaluation of these radiotracers in humans and/or monkeys showed that they are good candidates for imaging the SERT sites.

We hereby report the synthesis, in vitro characterization, radiosynthesis, in vivo regional brain distribution in rats of [^{123}I]ZIET and microPET imaging in nonhuman primates of [^{11}C]ZIET and [^{11}C]ZBrET. The development of these radiotracers as well as [^{123}I]ZIET was based on previous work with tropane derivatives with unsaturated functional groups in the 4′-position of the phenyl ring. A series of nortropanes was reported containing alkenyl substituents at the 4′-position of the phenyl ring of 2β-carbomethoxy-3β-arylnortropanes.[26,27] In this series, the cis and trans propenyl derivatives were potent and selective for the SERT versus the DAT in vitro. Goodman and colleagues[28] prepared and evaluated the 2-iodoethenyl derivative, 2β-carbomethoxy-3β-[4′-((*Z*)-2- iodoethenyl)phenyl]nortropane (ZIENT), which possessed very high affinity and selectivity for the hSERT as shown in Table 1. Additionally, SPECT imaging studies conducted with [^{123}I]ZIENT in monkeys demonstrated uptake of radioactivity in SERT-rich regions which was displaced with the selective SERT ligand, citalopram, demonstrating the potential of this tropane for visualizing the SERT.

Results and Discussion

Chemistry. ZIET and ZBrET were prepared from the same intermediate, the 2β-carbomethoxy-3β-(4′-bromophenyl)tropane (**2**) (Scheme 2). The synthesis of this compound was previously described as a four-step reaction processing through the conjugated addition of the phenyl ring, then nitration at the 4′-position of the ring, reduction of the nitro, and finally diazotation followed by treatment with cuprous bromide,[29] or as a two-step reaction involving the Grignard addition of 4-trimethylsilylphenylmagnesium bromide followed by bromodesilylation with *N*-bromosuccinimide.[30] In our hands, **2** was prepared directly by 1,4-addition of freshly made 4-bromophenylmagnesium bromide on the ecgnine methyl ester (**1**).[31] Tropane **2** was then converted to the 2β-carbomethoxy-3β-[4′-((*Z*)-2-trimethylstannylethenyl) phenyl]tropane (**3**) via a Stille coupling reaction using (*Z*)-1,2-trimethylstannylethylene[32] (**4**) and tetrakis(triphenylphosphine)palladium (0) as catalyst in toluene. This methodology was developed simultanously by Blough et al.[33] The tropane **3** was used as precursor in the radiosynthesis of [^{123}I]ZIET. ZIET and ZBrET were prepared by halodestannylation of **3** with iodine monochloride and *N*-bromosuccinimide, respectively. The preparation of [^{11}C]ZIET and [^{11}C]ZBrET, based on an *N*-methylation reaction, involved the synthesis of the corresponding desmethyl precursors 2β-carbomethoxy-3β-[4′-((*Z*)-2-iodoethenyl)phenyl]nortropane (ZIENT) and 2β-carbomethoxy-3β-[4′-((*Z*)-2-bromoethenyl)phenyl]nortropane (ZBrENT). Chronologically, the synthesis of ZIENT and ZBrENT was first carried out from aldehyde **5** (Scheme 3): ZIENT was prepared by treatment with triphenylphosphonium-iodomethylene ylid then cleavage of the Boc group.[28] Treatment of the aldehyde **5** with carbon tetrabromide and triphenylphosphine gave the *N*-(*tert*-butoxycarbonyl)-2β-carbomethoxy-3β-[4′-(2,2′-dibromo)ethenyl phenyl]nortropane (**6**) which was converted to ZBrENT by palladium-catalyzed hydrogenolysis using tetrakis-(triphenylphosphine)palladium (0) and tributyltin hydride[34] followed by deprotection of the amine. Most recently, ZIENT and ZBrENT were prepared from **2** according to an improve reaction sequence outlined in Scheme 4. The conversion of compound **2** to its corresponding carbamate using trichloroethylchloroformate followed by Zn−acetic acid reduction gave the nortropane **10**, from which were obtained ZIENT and ZBrENT

Scheme 2[a]

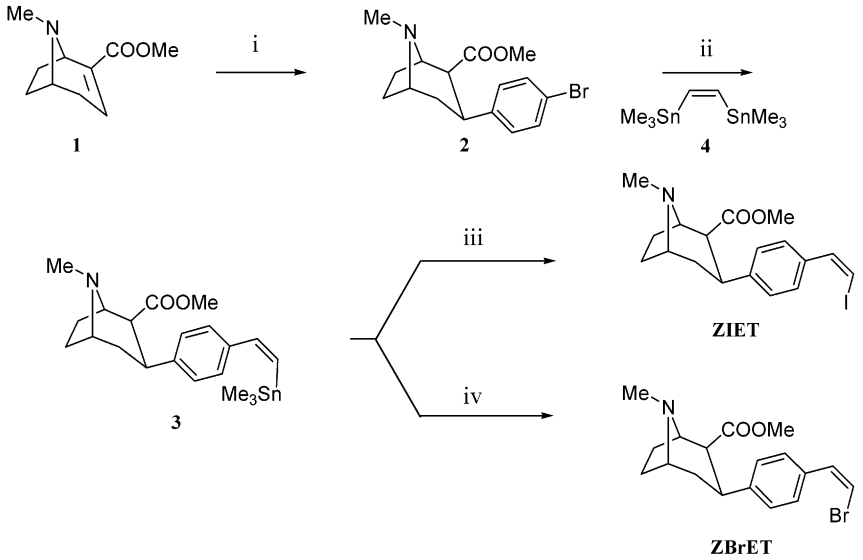

[a] Reagents: (i) 4-BrPhMgBr, −40 °C then TFA, −78 °C. (ii) **4**, $Pd(PPh_3)_4$, toluene, 100 °C. (iii) ICl, DCM, rt. (iv) NBS, DCM, rt.

Scheme 3[a]

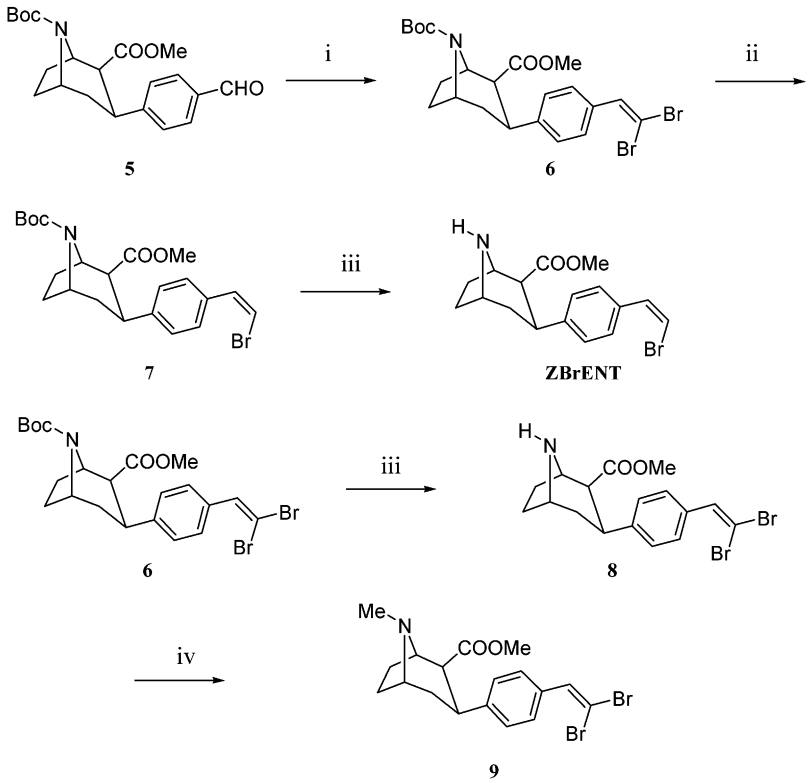

[a] Reagents: (i) CBr_4, PPh_3, DCM. (ii) n-Bu_3SnH, $Pd(PPh_3)_4$, toluene. (iii) TFA, DCM. iv) MeI, DMF, 90 °C.

according to the same pathway described above. To evaluate the binding potency of the 2β-carbomethoxy-3β-[4′-(2,2′-dibromo)ethenylphenyl]nortropane (**8**) and its *N*-methyl analogue **9**, the dibromo derivative **6** was hydrolyzed using trifluoroacetic acid in dichloromethane and the resulting nortropane **8** was alkylated with methyl iodide in *N*,*N*-dimethylformamide to afford the 2β-carbomethoxy-3β-[4′-(2,2′-dibromo)ethenylphenyl]-tropane (**9**) (Scheme 3).

Radiochemistry. The preparation of [^{11}C]ZIET and [^{11}C]ZBrET was accomplished through *N*-alkylation of the nortropane precursors, ZIENT and ZBrENT, with [^{11}C]CH_3I in *N*,*N*-dimethylformamide as shown in Scheme 5. The entire procedure required approximately 45 min from the end of bombardment. Productions of [^{11}C]labeled tropanes provided an average 30% decay-corrected yield ([^{11}C]ZIET: $n = 18$, [^{11}C]ZBrET: $n = 20$). Analytical HPLC demonstrated that the radiolabeled products were over 99% radiochemically pure and the specific activity of the products was ranging from 0.4 to 0.6 Ci/μmol at time of injection (3.4 to 5.2 Ci/μmol decay-corrected to end-of-bombardment).

The radioiodinated 2β-carbomethoxy-3β-[4′-((*Z*)-2-[^{123}I]iodoethenyl)phenyl]tropane [^{123}I]ZIET was prepared by treating the tin precursor **3** with $^{123}I^+$, generated from no-carrier-added Na[^{123}I]I and hydrogen

Scheme 4[a]

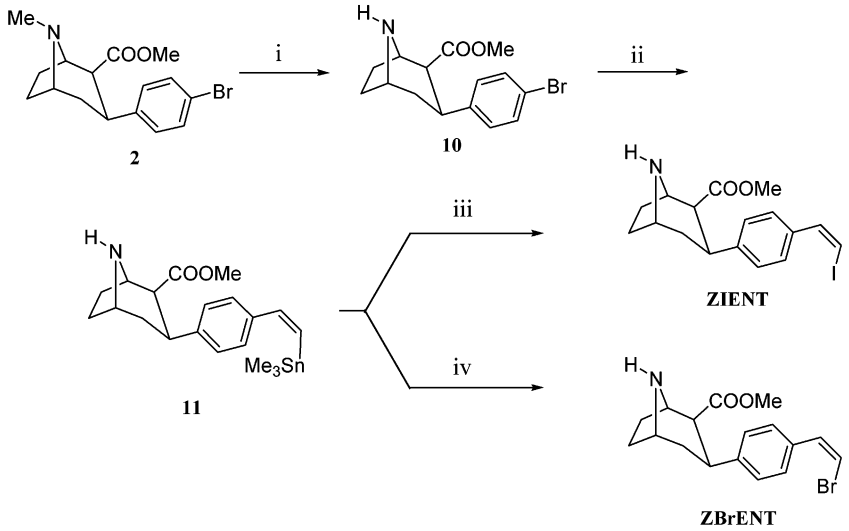

[a] Reagents: (i) TrocCl, toluene, reflux then Zn, AcOH, rt. (ii) (*Z*)-$Me_3SnCH{=}CHSnMe_3$, $Pd(PPh_3)_4$, toluene, 100 °C. (iii) ICl, DCM, rt. (iv) NBS, DCM, rt.

Scheme 5

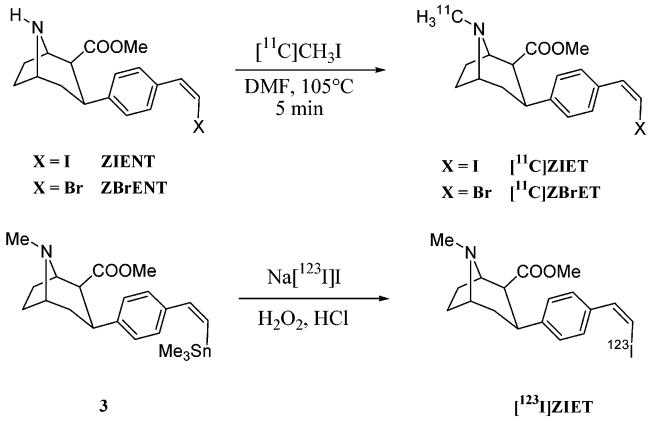

peroxide. The entire procedure required approximately 120 min. The radiolabeled product [^{123}I]ZIET was obtained in an average 33% decay-corrected yield (n = 2). The radiolabeled product was obtained in over 99% chemical and radiochemical purity, as demonstrated by analytical HPLC of the formulated solution. The specific activity of the product at time of injection was over 3.8 Ci/μmole.

Biological Results. In Vitro Competition Assays. The affinities of tropanes (ZIET, ZBrET and **9**) and nortropanes (ZIENT, ZBrENT and **8**) for the hSERT, hDAT, and hNET were determined through in vitro competition assays. These data are shown in Table 1 along with the previously determined K_i values for ZIENT.

[^{3}H]Citalopram (SERT ligand), [^{125}I]RTI-55 (DAT ligand), and [^{3}H]nisoxetine (NET ligand) were used as radiotracers during the in vitro displacement experiments. The rank of order of hSERT affinities was ZBrENT ≥ ZIENT > ZBrET ≥ **8** > ZIET > nor-β-CIT > **9** > β-CIT > RTI-113. As previously reported in the literature,[35] these results indicate that nortropanes have higher affinities for the hSERT than their corresponding tropanes. The rank of order of hDAT affinities was nor-β-CIT > β-CIT > RTI-113 > ZBrET ≥ ZBrENT > **8** > **9** > ZIENT > ZIET. In comparison with the hSERT affinities, the hDAT binding affinities of the 3β-[4′-(haloethenyl)phenyl]nortropanes and their associated *N*-methyltropanes are approximately the same and ranged from 3.5 to 6.7 nM. The measured binding affinity of ZIET for hDAT was significantly lower with a K_i of 22 nM. Consequently, the nortropanes exhibited a higher selectivity for the hSERT versus hDAT than corresponding tropanes. Nevertheless, ZBrET and especially ZIET showed higher affinity for the hSERT than the hDAT. The affinity for the hDAT of ZBrET and ZIET was 38- and 200-fold lower, respectively, than for the hSERT. These analyses demonstrated that ZIET and ZBrET possess high affinity and selectivity for hSERT versus hDAT and hNET and that bromo derivatives ZBrET and ZBrENT have higher affinities for both hSERT and hDAT than their iodo analogues.

Table 2. Brain Distribution of Activity in Sprague−Dawley Rats after iv Injection of [^{123}I]ZIET[a]

tissue	5 min	30 min	60 min	120 min
blood	0.45 ± 0.11	0.53 ± 0.03	0.43 ± 0.03	0.38 ± 0.02
hypothalamus	0.36 ± 0.13	0.68 ± 0.03	0.69 ± 0.06	0.60 ± 0.04
brainstem	0.35 ± 0.13	0.65 ± 0.02	0.54 ± 0.04	0.41 ± 0.02
cerebellum	0.34 ± 0.12	0.42 ± 0.01	0.27 ± 0.03	0.14 ± 0.02
frontal cortex	0.45 ± 0.16	0.82 ± 0.04	0.71 ± 0.06	0.48 ± 0.04
occipital cortex	0.45 ± 0.17	0.76 ± 0.04	0.63 ± 0.07	0.42 ± 0.05
striatum	0.39 ± 0.14	0.76 ± 0.03	0.71 ± 0.08	0.52 ± 0.03
hippocampus	0.38 ± 0.14	0.72 ± 0.03	0.63 ± 0.05	0.47 ± 0.03
rest of brain	0.38 ± 0.13	0.66 ± 0.03	0.54 ± 0.06	0.39 ± 0.03
thyroid	0.08 ± 0.03	0.74 ± 0.14	1.11 ± 0.16	2.12 ± 0.26

[a] Values are reported as the mean percent dose per gram of tissue ± standard error. n = 5 at all time points except at 120 min where n = 4.

Rodent Biodistribution Studies. A regional distribution study in the brain of male Sprague−Dawley rats was performed with iodine-123 labeled ZIET. [^{123}I]-ZIET allowed rodent studies to be conducted over a longer period of time and at higher specific activity than would be possible with [^{11}C]ZIET. The distribution of radioactivity was expressed as percent dose per gram in various tissues of brain male rats. The results shown in Table 2 demonstrated that the highest [^{123}I]ZIET uptake was observed at 30 min postinjection in all brain regions except the hypothalamus which showed the same activity of 0.69% dose/g at 60 min postinjection.

Table 3. Ratios of Uptake of Radioactivity in Various Brain Regions versus Cerebellum after iv Injection of [^{123}I]ZIET

brain region	5 min	30 min	60 min	120 min
hypothalamus	1.1	1.6	2.6	4.3
brainstem	1.0	1.5	2.0	3.0
frontal cortex	1.3	2.0	2.6	3.4
occipital cortex	1.3	1.8	2.3	3.0
striatum	1.1	1.8	2.6	3.7
hippocampus	1.1	1.7	2.3	3.4
rest of brain	1.1	1.6	2.0	2.8

Table 4. Brain Distribution of Activity in Sprague Dawley Rats 60 min after iv Injection of [^{123}I]ZIET in the Presence of Monoamine Transporter Ligands[a]

tissue	no blocker	citalopram	RTI-113	reboxetine
blood	0.22 ± 0.03	0.21 ± 0.01	0.24 ± 0.01	0.26 ± 0.01
hypothalamus	0.42 ± 0.11	0.20 ± 0.03	0.55 ± 0.07	0.46 ± 0.02
brainstem	0.33 ± 0.09	0.14 ± 0.02	0.35 ± 0.03	0.36 ± 0.02
cerebellum	0.15 ± 0.03	0.10 ± 0.02	0.13 ± 0.02	0.15 ± 0.01
frontal cortex	0.53 ± 0.13	0.21 ± 0.03	0.49 ± 0.06	0.47 ± 0.02
occipital cortex	0.46 ± 0.13	0.20 ± 0.04	0.42 ± 0.04	0.42 ± 0.02
striatum	0.42 ± 0.11	0.26 ± 0.04	0.45 ± 0.02	0.45 ± 0.01
hippocampus	0.40 ± 0.11	0.17 ± 0.02	0.42 ± 0.04	0.41 ± 0.02
rest of brain	0.37 ± 0.09	0.18 ± 0.02	0.36 ± 0.04	0.34 ± 0.01
thyroid	0.54 ± 0.11	0.93 ± 0.09	1.01 ± 0.03	1.12 ± 0.15

[a] Values are reported as the mean percent dose per gram of tissue ± standard error. $n = 3$ for the control group, $n = 4$ for the RTI-113 and citalopram group, and $n = 5$ for the reboxetine group. The monoamine transporter ligands were given 15 min prior to [^{123}I]ZIET at doses of 4 mg/kg.

The ratios of the uptake of radioactivity in the brain regions examined over time versus the cerebellum, a region with low density of serotonergic innervation, are shown in Table 3. At 120 min the highest ratios relative to the cerebellum were seen in the hypothalamus (4.3:1) and in the striatum (3.7:1). The brainstem, frontal cortex, occipital cortex, and hippocampus all demonstrated ratios greater than 3:1 at 120 min, while the remainder of the brain had a ratio of 2.8:1 at this time. The high uptake of [^{123}I]ZIET in the SERT-rich regions and the 13−27% washout in the hypothalamus, brainstem, striatum, and hippocampus from 60 to 120 min demonstrate that [^{123}I]ZIET has potentially favorable kinetic properties for in vivo quantification and imaging of the SERT by SPECT.

To assess the in vivo selectivity of [^{123}I]ZIET for the SERT versus the DAT and the NET, blocking studies were performed using citalopram as a brain available SERT-selective ligand, RTI-113 as a DAT-selective ligand and reboxetine as a NET-selective ligand (Scheme 1, Table 1). In these studies, rats received the monoamine transporter ligand (4 mg/kg) 15 min prior to receiving [^{123}I]ZIET and were compared to a group that received only [^{123}I]ZIET (no blocker group). The rats were sacrified 60 min after injection of [^{123}I]ZIET. After dissection, the uptakes of radioactivity in different parts of the brain were determined. The data (Table 4, Figure 1) were analyzed via a two-way ANOVA, and p values were calculated using Tukey's test for all pairwise multiple comparisons. No significant differences were found between the no blocker, RTI-113, and reboxetine groups ($p > 0.93$), while the citalopram group was significantly different than these three groups ($p < 0.001$). Within the no blocker group, the %ID/g in the cerebellum was significantly lower than in the other brain regions studied ($p < 0.001$) which is in agreement with the expected regional distribution of SERT in rat brain. The same results were seen within both the RTI-113 and reboxetine groups ($p < 0.003$). In contrast, no significant differences were detected between any of the brain regions including the cerebellum in the citalopram group. In light of the results obtained with PET imaging using [^{11}C]ZIET discussed in the following section, the uptake of radioactivity in the striatum warrants further discussion. In the blocking study, pretreatment with citalopram decreased striatal uptake of activity relative to the RTI-113, reboxetine, and no blocker groups ($p = 0.002$, $p < 0.001$, and $p = 0.02$, respectively). This result indicates that a large component of striatal uptake of [^{123}I]ZIET is due to SERT binding. However, within the citalopram group, there was a trend toward a significantly higher %ID/g in the striatum relative to the cerebellum ($p = 0.058$) not observed in other brain regions. This observation suggests that another, non-SERT component of striatal uptake might be present. Importantly, the %ID/g values observed in the striatum were virtually identical between the RTI-113, reboxetine, and no blocker groups, suggesting that [^{123}I]ZIET did not have appreciable DAT binding in the rat striatum.

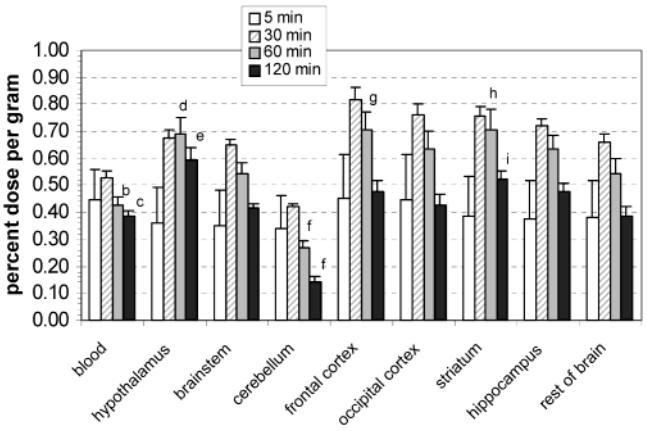

Figure 1. Brain distribution of activity in Sprague−Dawley rats after i.v. injection of [^{123}I]ZIET. [(a)] Values are reported as the mean percent dose per gram of tissue ± standard error. The data for the 60 and 120 min groups were analyzed separately using one-way ANOVAs with repeated measures, and p-values were calculated using Tukey's posthoc test for pairwise multiple comparisons. (b) Blood %ID/g at 60 min was less than hypothalamus ($p < 0.001$), brainstem ($p < 0.05$), frontal cortex ($p < 0.001$), occipital cortex ($p < 0.001$), striatum ($p < 0.001$), hippocampus ($p < 0.001$), and the rest of the brain ($p < 0.05$) at the same time point. Blood %ID/g at 60 min was greater than the cerebellum ($p < 0.001$) at the same time point. (c) Blood %ID/g at 120 min was less than hypothalamus ($p < 0.001$) and striatum ($p < 0.01$) at the same time point. Blood %ID/g at 120 min was greater than cerebellum ($p < 0.001$) at the same time point. (d) Hypothalamus %ID/g at 60 min was greater than brainstem ($p < 0.01$) and the rest of the brain ($p < 0.001$) at the same time point. (e) Hypothalamus %ID/g at 120 min was greater than brainstem ($p < 0.001$), frontal cortex ($p < 0.05$), occipital cortex ($p < 0.001$), hippocampus ($p < 0.05$), and the rest of the brain ($p < 0.001$) at the same time point. (f) Cerebellum %ID/g at 60 and 120 min was less than all other brain regions ($p < 0.001$ for all) at the same time points. (g) Frontal cortex %ID/g at 60 min was greater than the rest of the brain ($p < 0.001$) at the same time point. (h) Striatum %ID/g at 60 min was greater than the brainstem and the rest of the brain ($p < 0.001$ for both) at the same time point. (i) Striatum %ID/g at 120 min was greater than brainstem ($p < 0.05$) and the rest of the brain ($p < 0.01$) at the same time point.

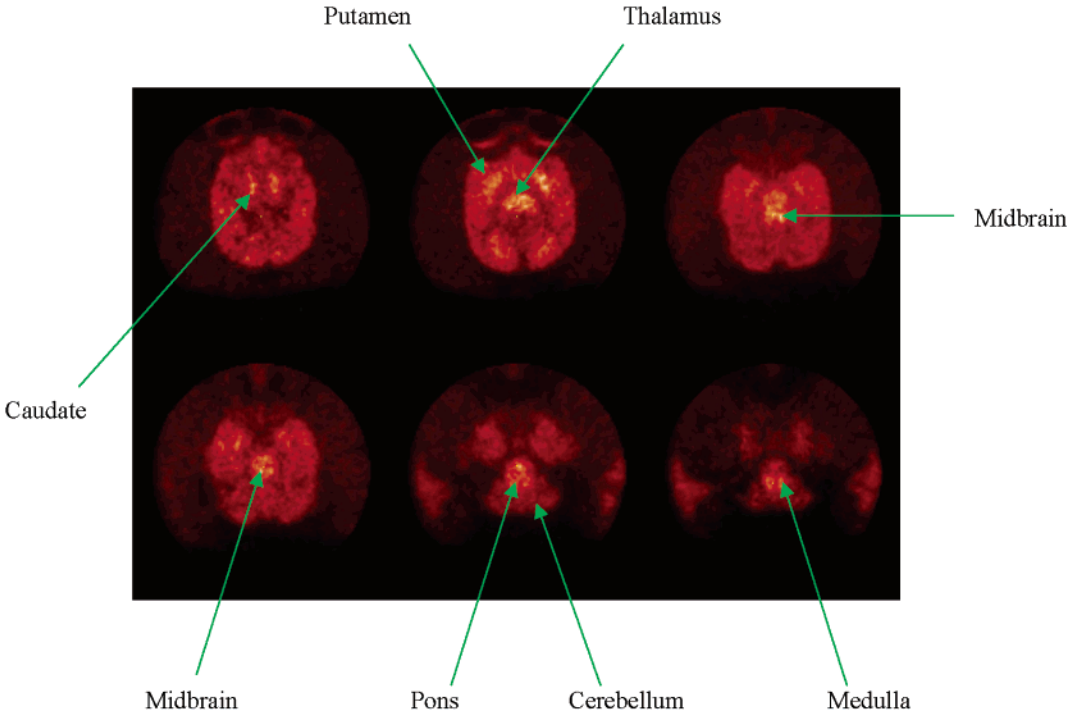

Figure 2. Transverse microPET images acquired using [^{11}C]ZIET.

In Vivo Nonhuman Primate Imaging. MicroPET imaging studies were performed with [^{11}C]ZIET and [^{11}C]ZBrET to assess the regional distribution, imaging properties and in vivo selectivity of these radioligands for the SERT in rhesus and cynomolgus monkeys. [^{11}C]-**9** was also evaluated in monkey and demonstrated a high nonspecific binding and a high uptake in the regions rich in DAT correlating its binding affinities (Table 1). This ligand did not warrant further investigations.

The microPET images acquired from 0 to 85 min using [^{11}C]ZIET and [^{11}C]ZBrET showed specific accumulation in the putamen, midbrain, thalamus, pons, medulla, and caudate as seen in Figures 2 and 3, respectively, with the lowest uptake occurring in the cerebellum. The corresponding time−activity curves describing the kinetics of [^{11}C]ZIET and [^{11}C]ZBrET binding in a rhesus monkey are presented in Figure 4 and Figure 5, respectively. The highest ratios relative to cerebellum occurred at the end of the study and were 2.3, 2.1, 2.1, 2.0, and 1.7 for the putamen, midbrain, pons, thalamus and medulla, respectively, when [^{11}C]-ZIET was injected and 2.3, 1.9, 1.8, 1.7, 1.6, and 1.3 for the putamen, midbrain, caudate, thalamus, pons, and medulla, respectively, when [^{11}C]ZBrET was injected. The higher ratios obtained with the more lipophilic [^{11}C]-ZIET compare to [^{11}C]ZBrET can be explained by its higher selectivity and slightly faster kinetics. The regional brain distribution of [^{11}C]ZIET and [^{11}C]ZBrET reflected the known distribution of SERT-rich sites in the brain. However, the uptake of radioactivity in the putamen, especially with [^{11}C]ZBrET, was slightly higher than in the midbrain and the thalamus. This distribution has not been observed with previously reported selective SERT imaging agents that have shown the highest levels of SERT in the midbrain and thalamus followed by intermediate level in the striatum, low levels in the cortexes and negligible levels in the cerebellum.[39,15] To assess the specificity of [^{11}C]ZIET and [^{11}C]ZBrET uptake, displacement studies were performed using the SERT ligand citalopram. A dose of citalopram (1.5 mg/kg) administered 40 min after injection of [^{11}C]ZIET and [^{11}C]ZBrET resulted in a significant reduction of radioactivity in the thalamus, midbrain, and pons in both cases (Figures 6 and 7) but no displacement from the putamen and the caudate suggesting that these tracers may bind to the DAT given the high DAT density of these regions. To assess the potential binding of [^{11}C]ZIET and [^{11}C]ZBrET to the DAT, chase studies were performed using 0.3 mg/kg of the DAT ligand RTI-113 administered 40 min after injection of radioactive tracer. In the study with [^{11}C]-ZBrET and RTI-113 acquired for a period of time of 85 min, no displacement of radioactivity from any part of the brain was observed (Figure 9). A slight displacement of [^{11}C]ZIET from the striatum was observed when RTI-113 was administered, with a percentage of washout of 4 and 5% from the caudate and putamen, respectively (Figure 8). However, if this slight decrease represents [^{11}C]ZIET binding to DAT sites, the administration of RTI-113 would be expected to displace the radioactivity uptake in the striatum because administration of citalopram did not chase any activity from this region of the brain. Similarly, RTI-113 has no effect on the [^{11}C]-ZBrET uptake, and yet ZBrET has a higher affinity for the DAT and less selectivity for the SERT than ZIET. Therefore, the inability of RTI-113 to significantly displace the radioactivity from the striatum suggests that [^{11}C]ZIET and [^{11}C]ZBrET bindings in the striatum is not due to reversible DAT binding. To confirm that the uptake of [^{11}C]ZIET or [^{11}C]ZBrET in the striatum was due to specific binding, a chase study using pharmacological doses of nonradioactive ZIET or ZBrET was performed. The administration of 0.3 mg/kg of ZIET or ZBrET 40 min after injection of the corresponding ^{11}C-labeled tropane demonstrated a significant reduction of

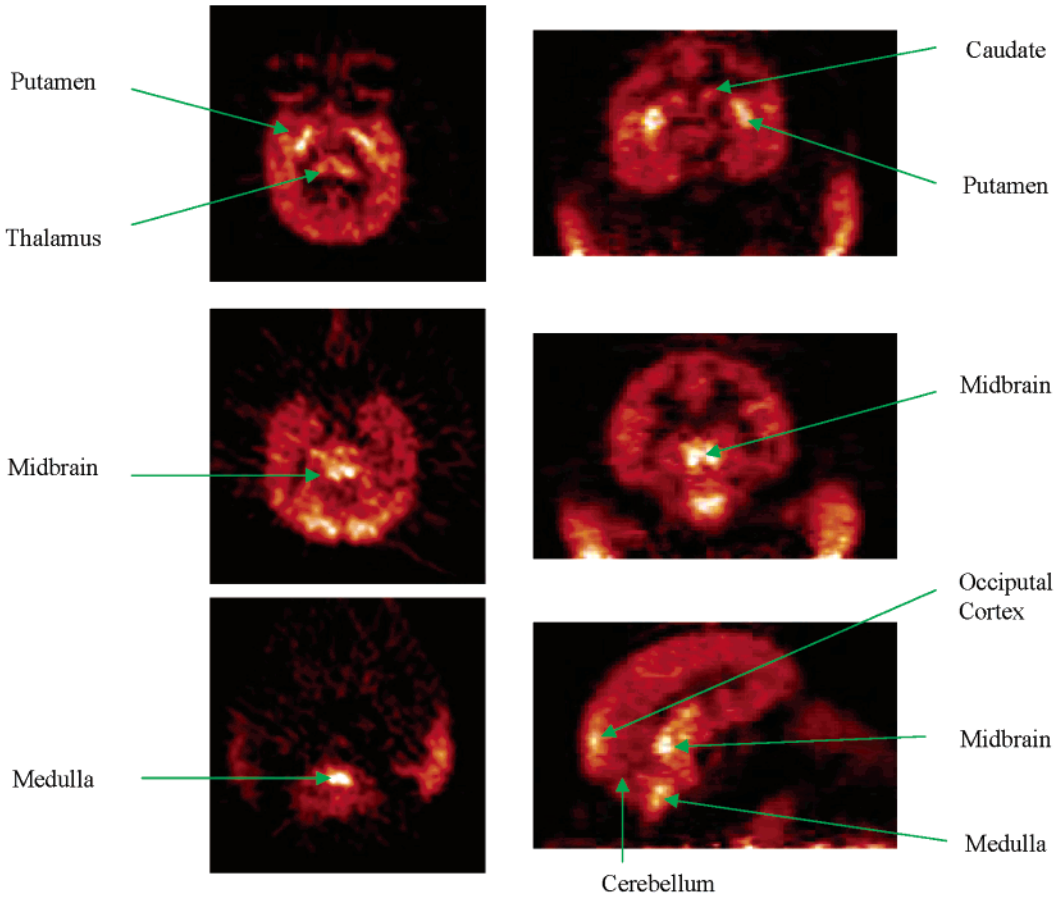

Figure 3. Transverse, coronal, and sagittal microPET images acquired using [^{11}C]ZBrET.

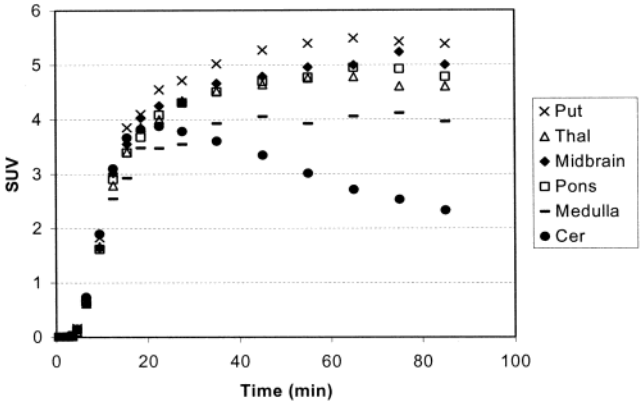

Figure 4. Time−activity curves for brain regions for [^{11}C]-ZIET in a rhesus monkey. Images were acquired for a total time of 85 min.

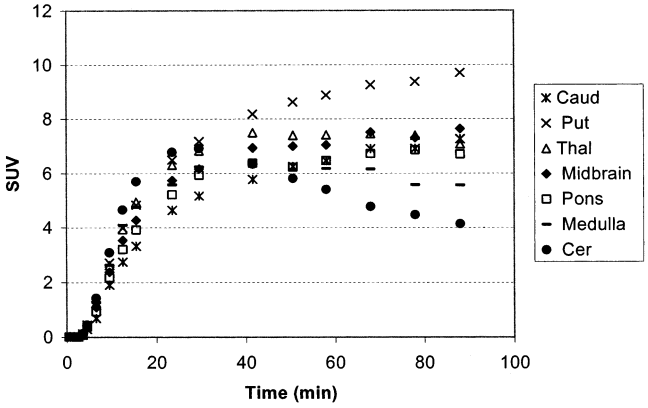

Figure 5. Time−activity curves for brain regions for [^{11}C]-ZBrET in a rhesus monkey. Images were acquired for a total time of 85 min.

radioactivity in the midbrain, putamen, caudate, thalamus, pons, and medulla. The percentages of washout of [^{11}C]ZIET were 35, 32, 30, 30, and 29% from the putamen, midbrain, thalamus, pons, and medulla, respectively, at 85 postinjection, and the percentages of washout of [^{11}C]ZBrET were 55, 49, 49, 49, 40, and 36% from the putamen, midbrain, thalamus, caudate, pons, and medulla, respectively, at 85 min postinjections (Figures 10 and 11). These studies indicate that radioactivity uptake in the striatum is primarily due to specific binding rather than nonspecific binding. To define the nature of [^{11}C]ZIET and [^{11}C]ZBrET uptake in the striatum, we performed a study in which the monkey was pretreated with 0.3 mg/kg of RTI-113, 30 min before injection of radioligand, followed, 40 min later by administration of 1.5 mg/kg of citalopram. The time−activity curves (Figures 12 and 13) demonstrate that the specific DAT ligand RTI-113 did not prevent the accumulation of radioactivity in the striatum, but unlike the previous citalopram studies, significant displacement from the putamen, caudate, thalamus, midbrain, pons, and medulla occurred. As seen in Figures 14 and 15, the same results were obtained when the monkeys were pretreated with citalopram (30 min prior to the injection of radioligand) and RTI-113 was administered 40 min postinjection. The accumulation of radioactivity in the striatum was not blocked by the presence of citalopram, but the radioactivity was displaced from this region by RTI-113. The logical next study was to inject simultaneously RTI-113 and citalo-

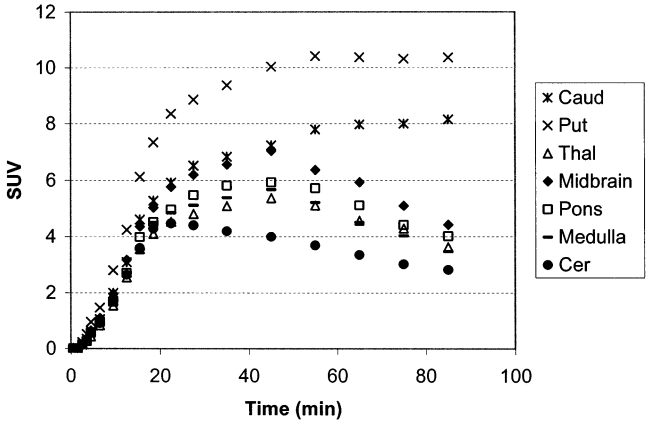

Figure 6. Time−activity curves for brain regions for [^{11}C]-ZIET in a cynomolgus monkey with citalopram administered at 40 min. Images were acquired for a total time of 85 min.

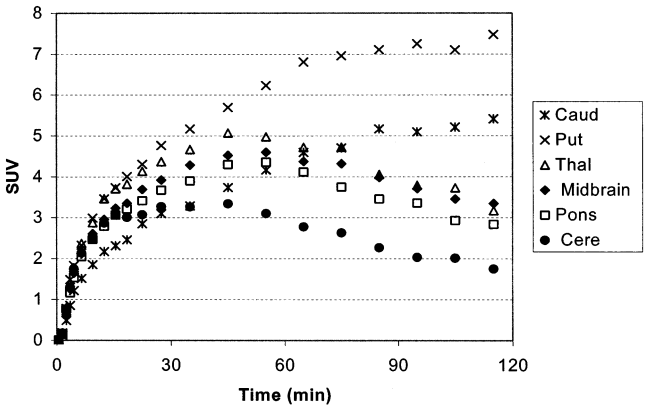

Figure 7. Time−activity curves for brain regions for [^{11}C]-ZBrET in a rhesus monkey with citalopram administered at 40 min. Images were acquired for a total time of 115 min.

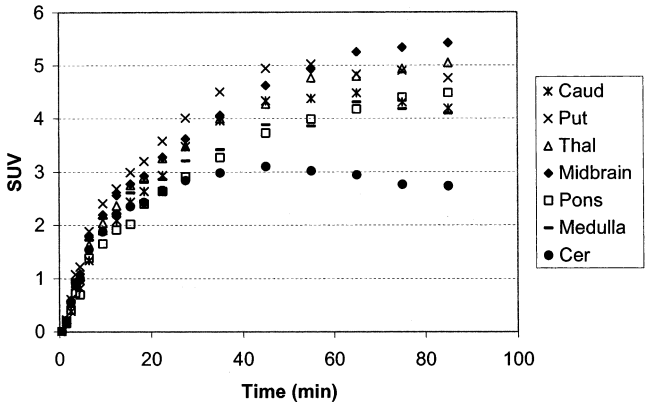

Figure 8. Time−activity curves for brain regions for [^{11}C]-ZIET in a cynomolgus monkey with RTI-113 administered at 40 min. Images were acquired for a total time of 85 min.

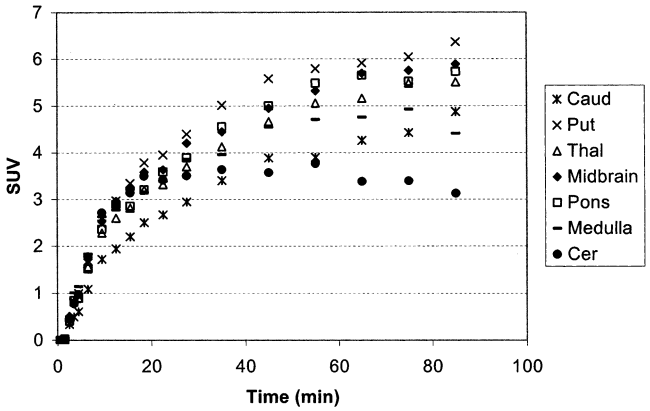

Figure 9. Time−activity curves for brain regions for [^{11}C]-ZBrET in a rhesus monkey with RTI-113 administered at 40 min. Images were acquired for a total time of 85 min.

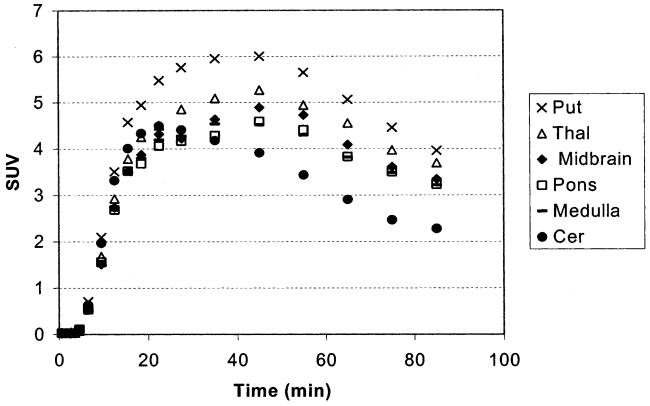

Figure 10. Time−activity curves for brain regions for [^{11}C]-ZIET in a rhesus monkey with ZIET administered at 40 min. Images were acquired for a total time of 85 min.

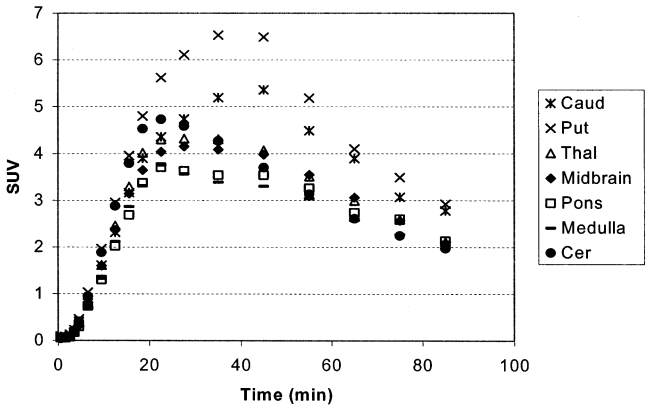

Figure 11. Time−activity curves for brain regions for [^{11}C]-ZBrET in a rhesus monkey with ZBrET administered at 40 min. Images were acquired for a total time of 85 min.

pram. These experiments carried out by injecting a mix consisting of 0.3 mg/kg of RTI-113 and 1.5 mg/kg of citalopram 80 min after the injection of [^{11}C]ZIET and [^{11}C]ZBrET showed a dramatic reduction of radioactivity from the SERT-rich regions including the striatum (Figures 16 and 17). These dual-administration studies indicate that uptake of radioactivity can be displaced from the striatum when both SERT and DAT sites are occupied.

Lipophilicity. The lipophilicities of ZIET and ZBrET were measured using the procedure of Wilson et al.[40] The measured log $P_{7.4}$ values for ZIET and ZBrET were 1.5 and 1.3, respectively. The initial brain uptake of CNS radioligands has been reported to be optimum when log $P_{7.4} = 2.4-2.8$.[41] Our radiotracer's values were below the optimal range; nonetheless, both [^{11}C]ZIET and [^{11}C]ZBrET achieved brain penetrance and good specific (midbrain) to nonspecific binding (cerebellum) ratios (2.1:1 and 1.9:1, respectively) at 85 min postinjection.

Metabolite Analysis in Monkeys. Arterial plasma samples from rhesus monkeys following antecubital vein injection of [^{11}C]ZIET and [^{11}C]ZBrET were analyzed for nonpolar, potentially brain permeable, metabolites

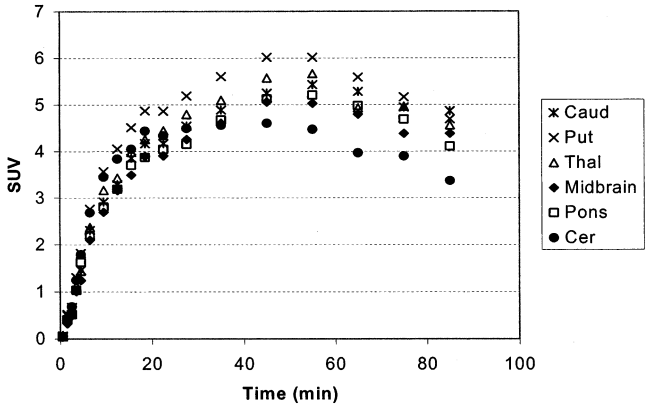

Figure 12. Time−activity curves for brain regions for [^{11}C]-ZIET in a rhesus monkey with RTI-113 administered 100 min prior injection of [^{11}C]ZIET and citalopram administered at 40 min. Images were acquired for a total time of 85 min.

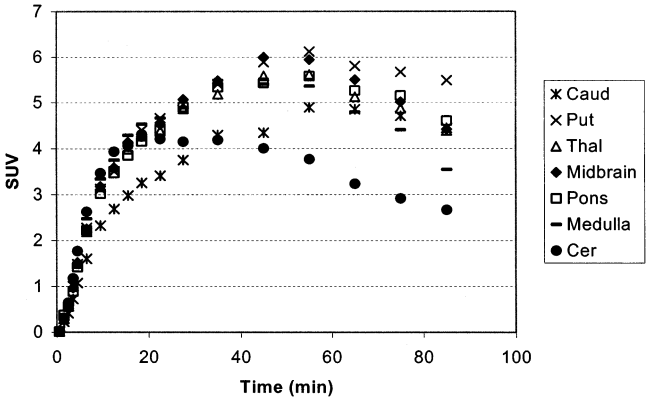

Figure 13. Time−activity curves for brain regions for [^{11}C]-ZBrET in a rhesus monkey with RTI-113 administered 100 min prior injection of [^{11}C]ZBrET and citalopram administered at 40 min. Images were acquired for a total time of 85 min.

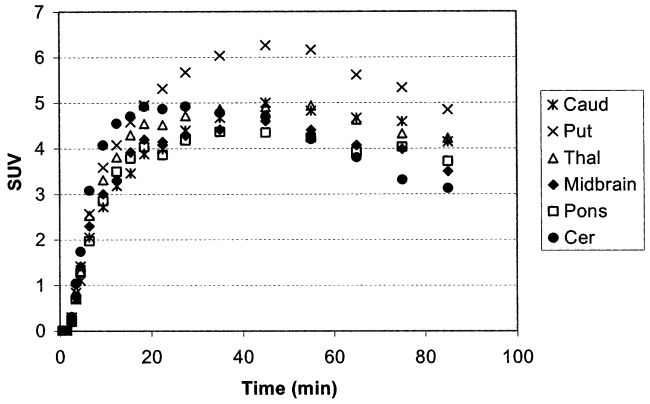

Figure 14. Time−activity curves for brain regions for [^{11}C]-ZIET in a rhesus monkey with citalopram administered 30 min prior injection of [^{11}C]ZIET and RTI-113 administered at 40 min. Images were acquired for a total time of 85 min.

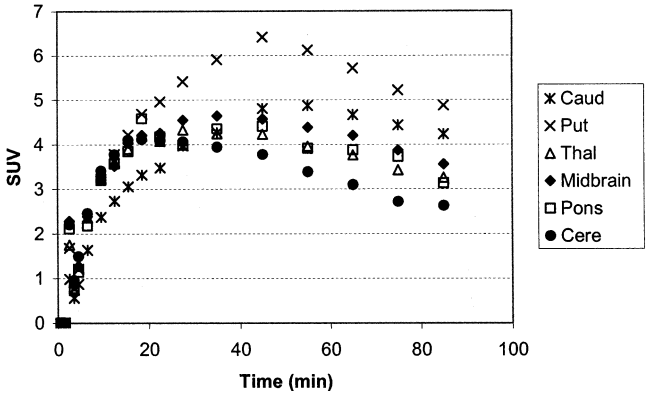

Figure 15. Time−activity curves for brain regions for [^{11}C]-ZBrET in a rhesus monkey with citalopram administered 30 min prior injection of [^{11}C]ZBrET and RTI-113 administered at 40 min. Images were acquired for a total time of 85 min.

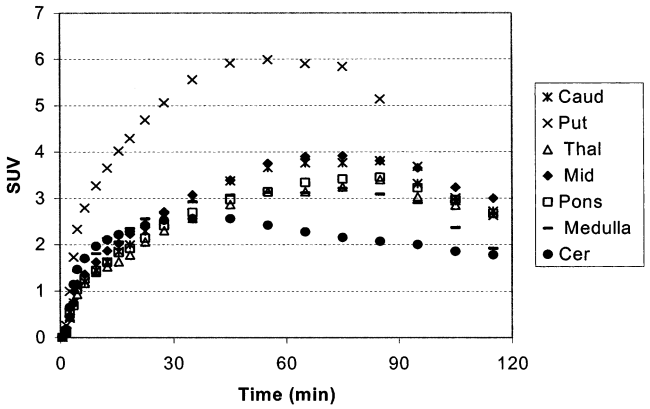

Figure 16. Time−activity curves for brain regions for [^{11}C]-ZIET in a rhesus monkey with a mix of citalopram and RTI-113 administered at 80 min. Images were acquired for a total time of 115 min.

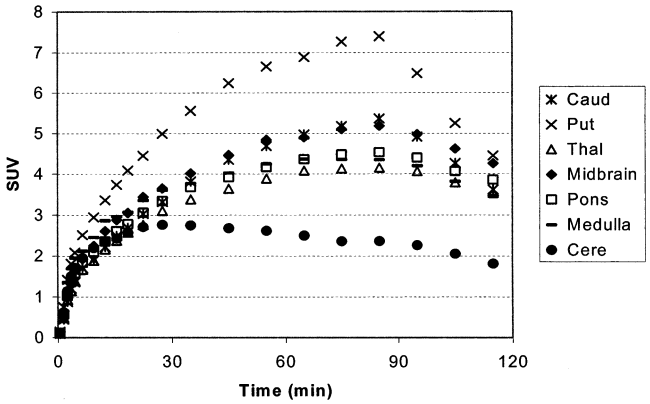

Figure 17. Time−activity curves for brain regions for [^{11}C]-ZBrET in a cynomolgus monkey with a mix of citalopram and RTI-113 administered at 80 min. Images were acquired for a total time of 115 min.

by a HPLC method. For both radiotracers, the major radioactive component appearing in the initial arterial plasma samples displayed a major peak on HPLC spectra corresponding to unmetabolized authentic [^{11}C]-ZIET and [^{11}C]ZBrET. The fraction of plasma radioactivity corresponding to unmetabolized [^{11}C]ZIET or [^{11}C]ZBrET rapidly decreased from 69% at 5 min to 12% at 40 min for [^{11}C]ZIET and from 63% at 5 min to 14.5% at 40 min for [^{11}C]ZBrET. The major radioactive metabolite found in arterial plasma using HPLC separation and gamma-counter detection was in both cases a more polar component. The abundance of the polar metabolite increased to 91% of the plasma activity by 80 min for [^{11}C]ZIET and 89% by 80 min for [^{11}C]ZBrET. The identity of the polar metabolites was not elucidated because they were not expected to enter the brain. In both cases, the metabolites were eluted immediately after the void volume and are probably the corresponding free acid. This hypothesis is based on our experience

with other tropanes and a plasma metabolite study reported in the literature[42] showing that the major metabolite obtained from [*N*-methyl-^{11}C]β-CIT was the [*N*-methyl-^{11}C]β-CIT acid which did not enter the brain in high quantity. The absence of labeled lipophilic metabolites in the arterial plasma that could reenter the brain permits uncorrected calculation of [^{11}C]ZIET and [^{11}C]ZBrET input functions and subsequent quantification of binding sites by tracer kinetic modeling without correcting for lipophilic metabolites.

Conclusion

Two new SERT ligands have been synthesized, radiolabeled, and evaluated in rats and nonhuman primates. Competition binding assays in cells stably expressing the human monoamine transporters demonstrated that ZIET and ZBrET have high affinities for the SERT. ZIET showed significantly higher selectivity for SERT over DAT than ZBrET, with ratios of 200 to 1, and 38 to 1, respectively. Biodistribution studies in rats showed that [^{123}I]ZIET uptake occurred specifically in regions rich in SERT. In vivo microPET imaging studies in monkeys demonstrated that [^{11}C]ZIET and [^{11}C]ZBrET exhibited high uptake in the striatum, diencephalon, and brainstem. However, a component of striatal uptake not displaceable by SERT or DAT ligands alone was observed. A series of a combination of blocking and displacement studies with RTI-113 and citalopram demonstrated that the component of striatal uptake of [^{11}C]ZIET was primarily SERT. These results support the candidacy of [^{11}C]ZIET and [^{123}I]ZIET for further study as radioligands for in vivo quantitation of SERT sites by PET and SPECT, respectively.

Experimental Section

All reagents used were obtained from commercially available sources. Solvents used in reactions were purchased from Aldrich Chemicals (Milwaukee, WI) while solvents for chromatography were obtained from VWR (West Chester, PA). Melting points are uncorrected and were determined in capillary tubes using a Mel-Temp II apparatus obtained from Laboratory Devices, Inc. (Holliston, MA). ^{1}H NMR spectra were recorded on a Varian spectrometer at 400 MHz or 300 MHz and referenced to the NMR solvent (chemical shifts in ppm values, *J* values in Hz). Mass spectra were determined on a VG 70-S double focusing mass spectrometer using high-resolution electron ionization (EI) or a JEOL JMS−SX102 double focusing mass spectrometer using fast atomic bombardment (FAB). Silica gel column chromatography was performed using Merck silica gel 60 (40−63 μm particle size). Thin-layer chromatography (TLC) was performed using 250 μm layers of F-254 silica on aluminum plates obtained from Whatman (Clifton, NJ).

Chemistry. 2β-Carbomethoxy-3β-(4′-bromophenyl)tropane (2). Magnesium chips (96 mg, 4 mmol) were stirred vigorously for 2 h under dry argon flow. Ether (0.6 mL) was added as well as a crystal of iodine. A solution of 1,4-dibromobenzene (1 g, 4 mmol) in ether (3.5 mL) was added dropwise in order to control and maintain the reflux. After completion of the addition, the reaction mixture was refluxed for 1 h then cooled to −40 °C. A solution of ecognine methyl ester (0.2 g, 1.1 mmol) in ether/dichloromethane (5 mL/5 mL) was added dropwise. The reaction mixture was stirred at −40 °C for 3 h then cooled to −70 °C and quenched with a solution of trifluoroacetic acid (0.45 mL, 5.8 mmol) in dichloromethane (2 mL). The reaction mixture was allowed to warm to −10 °C, and 5N HCl was added. The aqueous layer was retained, washed with ether, basified with (30% w/w) ammonium hydroxide, and extracted with dichloromethane. The yellow oil obtained was purified by flash chromatography (hexane: ethyl acetate:triethylamine 75:21:4) to give a white solid (155 mg, 41%). Spectroscopic and physical data were identical to those previously reported.[29]

2β-Carbomethoxy-3β-[4′-((*Z*)-2-trimethylstannylethenyl)phenyl]tropane (3). To a solution of 2β-carbomethoxy-3β-(4′-bromophenyl)tropane (**2**) (214 mg, 0.63 mmol) in toluene (10 mL) were added tetrakis(triphenylphosphine)palladium (0) (44 mg, 0.04 mmol) and (*Z*)-1,2-trimethylstannylethylene (**4**) (0.3 g, 0.78 mmol). The reaction mixture was stirred at 90 °C for 3 h. The toluene was removed under reduced pressure, and the black residue was purified by flash chromatography (hexane:ethyl acetate:triethylamine 80:18.5:1.5) to afford a yellow solid (160 mg, 57%). ^{1}H NMR ($CDCl_3$, 400 MHz) δ −0.01−0.01 (m. 9H), 1.60−1.76 (m, 3H), 2.08−2.14 (m, 1H), 2.17−2.24 (m, 1H), 2.24 (s, 3H), 2.56−2.63 (m, 1H), 2.90−2.92 (m, 1H), 2.99−3.05 (m, 1H), 3.37−3.41 (m, 1H), 3.46 (s, 3H), 3.53−3.57 (m, 1H), 6.13 (d, J = 13.6 Hz, 1H), 7.14−7.20 (m, 4H), 7.52 (d, J = 13.6 Hz, 1H). ^{13}C NMR ($CDCl_3$, 100 MHz) δ −7.87 (3C), 25.29, 26.19, 33.62, 34.09, 42.11, 51.37, 53.13, 62.47, 65.48, 127.10 (2C), 127.25 (2C), 132.98, 138.82, 142.51, 147.35, 172.35. HRMS (FAB) calcd for $C_{21}H_{32}NO_2Sn$ (^{120}Sn) [MH^+]: 450.1455, found 450.1460.

(*Z*)-1,2-Trimethylstannylethylene (4). To a solution of hexamethylditin (0.49 g, 1.37 mmol) in 5 mL of 1,4-dioxane was added tetrakis(triphenylphosphine)palladium(0) (80 mg, 0.07 mmol). The reaction mixture was warmed at 60−65 °C, and purified acetylene (passed successively through the following traps: cold trap at −78 °C, concentrated sulfuric acid, solid potassium hydroxide, and Drierite) was bubbled through the reaction mixture. After a few minutes, the reaction mixture turned black. After 2 h the reaction was complete, and the volatiles were evaporated under reduce pressure. Purification by flash chromatography (hexane + 0.2% triethylamine) gave a yellow oil (260 mg, 49%) which was used without any further purification.

2β-Carbomethoxy-3β-[4′-((*Z*)-2-iodoethenyl)phenyl]tropane (ZIET). To a solution of 2β-carbomethoxy-3β-[4′-((*Z*)-2-trimethylstannylethenyl)phenyl]tropane (**3**) (0.390 g, 0.87 mmol) in dichloromethane (15 mL) at 25 °C was added dropwise iodine monochloride (1 M in dichloromethane, 0.85 mL). The reaction mixture was stirred for 10 min and then quenched with an aqueous solution of sodium metabisulfite (5% w/w, 10 mL). The organic layer was separated, washed with water, and evaporated under reduced pressure. Purification by flash chromatography (hexane:ethyl acetate:triethylamine 80:18.5:1.5) afforded a yellow oil (0.261 g, 73%). Additional purification by HPLC was performed to obtain the pure standard for labeling (Waters, X-terra RP_{18} 7.8 × 100 mm, 35% H_2O in methanol + 0.1% Et_3N, 3 mL/min, t_R = 10.2 min). ^{1}H NMR ($CDCl_3$, 400 MHz) δ 1.58−1.77 (m, 3H), 2.10−2.22 (m, 2H), 2.21 (s, 3H), 2.59−2.71 (m, 1H), 2.94−3.09 (m, 2H), 3.41−3.46 (m, 1H), 3.51 (s, 3H), 3.59−3.63 (m, 1H), 6.48 (d, J = 8.4 Hz, 1H), 7.25−7.28 (m, 3H), 7.57 (d, J = 8.0 Hz, 2H). ^{13}C NMR (100 MHz) δ 25.36, 26.09, 33.86, 34.10, 42.16, 51.38, 52.84, 62.40, 65.49, 78.15, 127.23 (2C), 128.24 (2C), 134.21, 138.51, 143.82, 172.30. HRMS (EI) calcd for $C_{18}H_{22}NIO_2$: 411.0695. Found: 411.0688. HPLC Waters Nova-Pak C_{18} column 3.9 × 150 mm, absorbance wavelength: 254 nM, eluent A: 30% H_2O in MeOH + 0.1% NEt_3, 1 mL/min, t_R = 12.27 min, eluent B: 30% H_2O in CH_3CN + 0.1% NEt_3, 1 mL/min, t_R = 4.02 min.

2β-Carbomethoxy-3β-[4′-((*Z*)-2-bromoethenyl)phenyl]tropane (ZBrET). To a solution of 2β-carbomethoxy-3β-[4′-((*Z*)-2-trimethylstannylethenyl)phenyl]tropane (**3**) (0.110 g, 0.245 mmol) in dichloromethane (7.5 mL) at 25 °C was added *N*-bromosuccinimide (49 mg, 0.272 mmol). The reaction mixture was stirred for 10 min and then quenched with an aqueous solution of sodium metabisulfite (5% w/w, 10 mL). The organic layer was separated, washed with water, and evaporated under reduced pressure. Purification by flash chromatography (hexane:ethyl acetate:triethylamine 80:18.5:1.5) afforded a yellow oil (0.063 g, 70%). Additional purification by HPLC was performed to obtain the pure standard for

labeling (Waters, X-terra RP_{18} 7.8 × 100 mm, 35% H_2O in methanol + 0.1% Et_3N, 3 mL/min, t_R = 8.2 min). ^1H NMR ($CDCl_3$, 300 MHz) δ 1.57−1.77 (m, 3H), 1.97−2.26 (m, 2H), 2.24 (s, 3H), 2.55−2.65 (m, 1H), 2.91−3.04 (m, 2H), 3.38−3.40 (m, 1H), 3.50 (s, 3H), 3.56−3.59 (m, 1H), 6.35 (d, J = 8.1 Hz, 1H), 7.00 (d, J = 8.1 Hz, 1H), 7.26 (d, J = 8.4 Hz, 2H), 7.61 (d, J = 8.4 Hz, 2H). ^{13}C NMR (CD_3OD, 100 MHz) δ 25.69, 26.65, 34.62, 34.76, 42.00, 51.80, 53.51, 63.88, 66.56, 106.28, 128.29, 129.92, 133.42, 134.29, 144.54, 174.12. HRMS (EI) calcd for $C_{18}H_{22}BrNO_2$ (^{79}Br): 363.0834. Found: 363.0837 (Int: 95%), calcd for $C_{18}H_{22}BrNO_2$ (^{81}Br): 365.0813. Found: 365.0829 (Int: 100%). HPLC Waters Nova-Pak C_{18} column 3.9 × 150 mm, absorbance wavelength: 254 nM, eluent A: 30% H_2O in MeOH + 0.1% NEt_3, 1 mL/min, t_R = 12.21 min, eluent B: 30% H_2O in CH_3CN + 0.1% NEt_3, 1 mL/min, t_R = 4.47 min.

***N*-(*tert*-Butoxycarbonyl)-2β-carbomethoxy-3β-[4′-formylphenyl]nortropane (5).** Protocol and spectroscopic and physical data were identical to those previously reported.[28]

***N*-(*tert*-Butoxycarbonyl)-2β-carbomethoxy-3β-[4′-(2,2′-dibromo)ethenylphenyl]nortropane (6).** To a solution of carbon tetrachloride (94 mg, 0.28 mmol) in dichloromethane (1.5 mL) at −5 °C was added dropwise a solution of triphenylphosphine (149 mg, 0.57 mmol) in dichloromethane (1.5 mL). The resulting yellow solution was stirred for 10 min at −5 °C, then the aldehyde **5** (53 mg, 0.14 mmol) dissolved in dichloromethane (1.5 mL) was added dropwise. The reaction mixture was stirred for 25 min at 25 °C. The reaction mixture was diluted with dichloromethane and washed with a solution of ammonium hydroxide (5% w/w). The organic layer was dried over anhydrous magnesium sulfate and evaporated. Purification by flash chromatography (hexane:ethyl acetate 75:25) gave a yellow oil (63 mg, 84%). ^1H NMR ($CDCl_3$, 400 MHz) δ 1.42 and 1.46 (s, 9H), 1.65−1.85 (m, 3H), 2.0−2.18 (m, 2H), 2.74−2.77 (m, 1H), 2.87−2.92 (m, 1H) 3.2−3.27 (m, 1H), 3.44 (s, 3H), 4.42−4.68 (m, 2H), 7.20−7.26 (m, 2H), 7.41 (s, 1H), 7.46 (d, J = 8.4 Hz).

***N*-(*tert*-Butoxycarbonyl)-2β-carbomethoxy-3β-[4′-((*Z*)-2-bromoethenyl)phenyl]nortropane (7).** To a degassed solution of *N*-(*tert*-Butoxycarbonyl)-2β-carbomethoxy-3β-[4′-(2,2′-dibromo)ethenylphenyl]nortropane (**6**) (62 mg, 0.117 mmol) in dry toluene (2.5 mL) were added tetrakis(triphenylphosphine)palladium (0) (6 mg, 0.005 mmol) then a solution of tributyltin hydride (35 mg, 0.13 mmol) in toluene (0.5 mL). The reaction mixture was stirred for 1 h at 25 °C, then diluted with dichloromethane and washed with water. Purification by flash chromatography (hexane:ethyl acetate 75:25) gave an oil (50 mg). ^1H NMR ($CDCl_3$) showed that the product obtained contains 5% of dehalogenated compound.

2β-carbomethoxy-3β-[4′-(2,2′-dibromo)ethenylphenyl]nortropane (8). To a solution of *N*-(*tert*-butoxycarbonyl)-2β-carbomethoxy-3β-[4′-(2,2′-dibromo)ethenylphenyl]nortropane (**6**) (23 mg, 0.043 mmol) in dichloromethane (1.5 mL) at −5 °C was added dropwise trifluoroacetic acid (0.15 mL). The reaction mixture was stirred for 45 min at 25 °C. The solvent and reagent were evaporated under reduced pressure. The residue was dissolved in dichloromethane and washed with ammonium hydroxide (5% w/w). Purification by HPLC (Waters, Novapak C_{18} semiprep 25 × 100 mm, 20% H_2O in methanol + 0.1% Et_3N, 6 mL/min, t_R = 31.0 min) gave a thick oil (13 mg, 70%).^1H NMR ($CDCl_3$, 400 MHz) δ 1.61−1.80 (m, 3H), 1.98−2.18 (m, 2H), 2.30−2.65 (br s, 1H), 2.38−2.45 (m, 1H), 2.74−2.79 (m, 1H), 3.20−3.27 (m, 1H), 3.73 (s, 3H), 3.71−3.76 (m, 2H), 7.19 (d, J = 8.0 Hz, 2H), 7.43 (s, 1H), 7.46 (d, J = 8.0 Hz, 2H). HRMS (FAB) calcd for $C_{17}H_{20}O_2NBr_2$ (2 ^{79}Br) [MH^+]: 427.9861. Found: 427.9852 (Int: 52.6%), calcd for $C_{17}H_{20}O_2NBr_2$ (1 ^{79}Br + 1 ^{81}Br) [MH^+]: 429.9840. Found: 429.9836 (Int: 100.0%), calcd for $C_{17}H_{20}O_2NBr_2$ (2 ^{81}Br) [MH^+]: 431.9820. Found: 431.9822 (Int: 49.2%).

2β-Carbomethoxy-3β-[4′-(2,2′-dibromo)ethenylphenyl]tropane (9). To a solution of 2β-carbomethoxy-3β-[4′-(2,2′-dibromo)ethenylphenyl]nortropane (6 mg, 0.014 mmol) in *N*,*N*-dimethylformamide (0.4 mL) was added 2 drops of methyl iodide. The reaction mixture was heated at 100 °C for 8 min then diluted with water (4 mL) and applied onto a C_{18} SepPak. The C_{18} SepPak was washed with water (40 mL) and the tropane was eluted with ethanol (3 mL). After evaporation of ethanol, the residue (5 mg) was purified by HPLC (Waters, X-terra RP_{18} 7.8 × 100 mm, 33% H_2O in methanol + 0.1% Et_3N, 4 mL/min, t_R = 7.3 min) to give an oil (3 mg, 48%). ^1H NMR ($CDCl_3$, 300 MHz) δ 1.54−1.75 (m, 3H), 2.06−2.34 (m, 2H), 2.27 (s, 3H), 2.55−2.68 (m, 1H), 2.87−3.45 (m, 2H), 3.38−3.50 (m, 1H), 3.50 (s, 3H), 3.56−3.65 (m, 1H), 7.25 (m, 1H), 7.42 (s, 1H), 7.46 (d, J = 8.1 Hz, 2H).

2β-carbomethoxy-3β-[4′-((*Z*)-2-trimethylstannylethenyl)phenyl]nortropane (11). To a solution of 2β-carbomethoxy−3β-(4′−bromophenyl)nortropane (**10**) (270 mg, 0.83 mmol) in toluene (13 mL) were added tetrakis(triphenylphosphine)-palladium(0) (58 mg, 0.05 mmol) and (*Z*)-1,2−trimethylstannylethylene (**4**) (0.45 g, 1.27 mmol). The reaction mixture was stirred at 90°C for 3 h. The toluene was removed under reduced pressure, and the black residue was purified by flash chromatography (hexane:ethyl acetate:triethylamine 65:30:5) to afford a yellow oil (188 mg, 52%). ^1H NMR ($CDCl_3$, 300 MHz) δ −0.04−0.14 (m, 9H), 1.60−2.19 (m, 6H), 2.38−2.48 (m, 1H), 2.74−2.77 (m, 1H), 3.21−3.29 (m, 1H), 3.37 (s, 3H), 3.68−3.75 (m, 2H), 6.16 (d, J = 8.8 Hz, 1H), 7.14 (d, J = 8.7 Hz, 2H), 7.18 (d, J = 8.7 Hz, 2H), 7.53 (d, J = 8.8 Hz, 1H). ^{13}C NMR ($CDCl_3$, 100 MHz) δ −7.89 (3C), 27.76, 29.22, 33.75, 35.59, 51.30, 51.38, 53.82, 56.47, 127.37 (4C), 133.52, 139.52, 141.67, 147.14, 174.09. HRMS (EI) calcd for $C_{20}H_{29}NO_2Sn$ (120Sn): 435.1220, found 435.1219.

2β-carbomethoxy-3β-[4′-((*Z*)-2-bromoethenyl)phenyl]-nortropane (ZBrENT). To a solution of 2β-carbomethoxy-3β-[4′-((*Z*)-2-trimethylstannylethenyl)phenyl]nortropane (**11**) (0.188 g, 0.43 mmol) in dichloromethane (20 mL) at 0 °C was added dropwise a solution of bromine (0.5 M in carbon tetrachloride, 1.0 mL). The reaction mixture was stirred at this temperature for 5 min, and then quenched with an aqueous solution of sodium metabisulfite (5% w/w, 10 mL). The organic layer was separated, washed with water, and evaporated under reduced pressure. Purification by flash chromatography (dichloromethane:methanol 95:5) afforded a yellow oil (0.11 g, 73%). The precursor for labeling was purified again by HPLC (Waters, X-terra RP_{18} 7.8 × 100 mm, 35% H_2O in methanol + 0.1% Et_3N, 3 mL/min, t_R = 7.1 min). ^1H NMR ($CDCl_3$, 400 MHz) δ 1.66−1.84 (m, 3H), 2.06−2.25 (m, 2H), 2.42−2.49 (m, 1H), 2.77−2.78 (m, 1H), 2.87 (br s, 1H), 3.24−3.30 (m, 1H), 3.38 (s, 3H), 3.78−3.85 (m, 2H), 6.39 (d, J = 8.0 Hz, 1H), 7.02 (d, J = 8.0 Hz, 1H), 7.19 (d, J = 8.4 Hz, 2H), 7.62 (d, J = 8.4 Hz, 2H). ^{13}C NMR ($CDCl_3$, 100 MHz) δ 27.31, 28.62, 33.15, 35.49, 50.57, 51.39, 53.71, 56.25, 106.13, 127.13 (2C), 128.99 (2C), 131.92, 133.36, 141.89, 173.83. HRMS (EI) calcd for $C_{17}H_{20}BrNO_2$ (^{79}Br): 349.0677. Found: 349.0678 (Int: 100%), calcd for $C_{17}H_{20}BrNO_2$ (^{81}Br): 351.0656. Found: 351.0633 (Int: 93%).

2β-Carbomethoxy-3β-[4′-((*Z*)-2-iodoethenyl)phenyl]nortropane (ZIENT). To a solution of 2β-carbomethoxy-3β-[4′-((*Z*)-2-trimethylstannylethenyl)phenyl]nortropane (**11**) (0.1 g, 0.23 mmol) in dichloromethane (10 mL) at 0 °C was added dropwise iodine monochloride (1 M in dichloromethane, 0.28 mL). The reaction mixture was stirred at this temperature for 7 min and then quenched with an aqueous solution of sodium metabisulfite (5% w/w, 10 mL). The organic layer was separated, washed with water, and evaporated under reduced pressure. Purification by flash chromatography (dichloromethane:methanol 95:5) afforded a yellow oil which was purified by HPLC (Waters, X-terra RP_{18} 7.8 × 100 mm, 35% H_2O in methanol + 0.1% Et_3N, 3 mL/min, t_R = 8.15 min) to give a thick oil (60 mg, 66%) that slowly crystallizes. ^1H NMR ($CDCl_3$, 400 MHz) δ 1.64−1.81 (m, 3H) 2.00−2.17 (m, 2H), 2.39−2.47 (m, 1H), 2.76−2.77 (m, 1H), 2.87 (br s, 1H), 3.23−3.29 (m, 1H), 3.38 (s, 3H), 3.72−3.79 (m, 2H), 6.52 (d, J = 8.4 Hz, 1H), 7.20 (d, J = 8.4 Hz, 2H), 7.27 (d, J = 8.4 Hz, 1H), 7.56 (d, J = 8.4 Hz, 2H). ^{13}C NMR ($CDCl_3$, 100 MHz) δ 27.84, 29.27, 33.73, 35.80, 51.15, 51.36, 53.79, 56.49, 78.97, 127.29 (2C), 128.50 (2C), 135.05, 138.42, 142.82, 173.99. HRMS (EI) calcd for $C_{17}H_{20}INO_2$: 397.0539, Found 397.0528.

Radiolabeling. No-carrier-added [^{11}C]CO_2 was produced through the bombardment of $^{14}N_2$ gas containing 1% $^{16}O_2$ by a Siemens 11 MeV RDS 112 cyclotron at Emory University Hospital through the ^{14}N[p,α]^{11}C reaction. Radiosyntheses employing [^{11}C]CH_3I utilized a GE MicroLab methyl iodide system for the conversion of [^{11}C]CO_2 to [^{11}C]CH_3I. The syntheses of [^{11}C]ZIET and [^{11}C]ZBrET were performed using the nortropane precursors, ZIENT and ZBrENT. The precursor (~ 0.5 mg) dissolved in *N*,*N*-dimethylformamide (250 μL) was placed in a sealed v-vial (1.0 mL). The [^{11}C]CH_3I was delivered as a gas to the reaction vial and bubbled through the solution containing the precursor with ice bath cooling. After delivery of [^{11}C]CH_3I, the sealed vessel was heated at 105 °C for 5 min. The reaction mix was diluted with HPLC mobile phase (500 μL) prior to injection onto the semiprep HPLC column. HPLC purification was performed using a reverse phase C_{18} column (Waters, NovaPak C_{18}, 25 × 100 mm) at a 9 mL/min flow rate with a buffered mobile phase consisting of 32% water in acetonitrile and containing 1.4 g of ammonium acetate per liter of solvent. At a flow rate of 9 mL/min, the retention time of [^{11}C]ZIET and [^{11}C]ZBrET were approximately 14 and 12 min, respectively, and fractions eluting at this time containing activity were purified using a modified solid-phase extraction (SPE) procedure based upon Lemaire's method.[43] The desired fractions were combined with an equal volume of a 6 mg/mL aqueous sodium carbonate solution. After stirring, the homogeneous solution was applied to a Waters C_{18} SepPak (previously activated with ethanol (10 mL) and water (10 mL)) by transferring under vacuum through a cook line. The eluate was directed to the waste.

The C_{18} SepPak was successively washed with saline (0.9% NaCl, 40 mL) and ethanol (0.5 mL) (all directed to the waste). The radiolabeled tropane was eluted with ethanol (1.5 mL) and driven to a sterile empty vial containing 3.5 mL of saline. The resulting solution was transferred under argon pressure through a Millipore filter (pore size 1.0 μm) followed by a smaller one (pore size 0.2 μm), to a 30 mL sterile vial containing 10 mL of saline. The total synthesis time (including purification and formulation) of [^{11}C]ZIET and [^{11}C]ZBrET labeling was approximately 45 min from end of bombardment. Radiochemical purity greater than 99% and specific activity of 0.4−0.6 Ci/μmol were demonstrated using reverse-phase analytical HPLC (NovaPak, 3.9 × 150 mm) at 1.0 mL/min flow rate with a mobile phase consisting of 70:30:0.1 methanol: water:triethylamine.

The synthesis of [^{123}I]ZIET was performed using no-carrier-added Na[^{123}I]I purchased from MDS Nordion, Inc. (Ottawa, ON Canada). The trimethyltin precursor **3** (100 μg) dissolved in ethanol (0.3 mL) was added to a sealed vial containing Na[^{123}I]I (~5 mCi) in 0.1 N sodium hydroxide (~10−30 μL). In rapid succession, an excess of 0.4 N aqueous hydrochloric acid (100 μL) was added followed by 3% hydrogen peroxide (50 μL). The reaction vial was inverted several times to mix the reagents, and the reaction was allowed to proceed at room temperature for 25 min. The reaction was quenched by the addition of aqueous sodium hydrogensulfate (0.25 g/mL, 50 μL), and the reaction mixture was drawn into a syringe containing an aqueous solution of saturated sodium bicarbonate (0.5 mL). The reaction mix was passed through a C_{18} SepPak (preconditioned with methanol (10 mL)), and the SepPak was eluted sequentially with water (3, 10, and 5 mL). The radiolabeled product was then eluted from the C_{18} SepPak with 1 mL portions of methanol which were collected as individual fractions. The methanol fractions containing significant activity (~five total fractions) were combined and evaporated at 65 °C with argon flow over the course of approximately 30 min. The residue was diluted with 0.4 mL of water prior to HPLC. Purification via HPLC was performed using an X-Terra column (Waters, Prep RP_{18} 7.8 × 100 mm, 5 μm particle size) at a 3.0 mL/min flow rate with a mobile phase consisting of 38% water in methanol + 0.1% of triethylamine. Under these conditions, the [^{123}I]ZIET product had a retention time of approximately 15 min. Fractions containing radioactivity eluting at the expected retention time were combined and subject to SPE formulation as described previously. A sample of the final product from each production was taken to determine the pH, the radiochemical purity and the specific activity of the final dose. The same analytical HPLC conditions used to assess doses of [^{11}C]ZIET were used for [^{123}I]-ZIET.

Lipophilicity Measurements. Measurement of distribution coefficients of radiolabeled compounds were performed based on the method described by Wilson et al. using 0.02 M sodium phosphate buffer at pH 7.4 and 1-octanol.[40] Each log $P_{7.4}$ determination was performed in quadruplicate for each radiotracer. A ~20 μCi portion of the radiotracer was added to 5 mL of the phosphate buffer and shaken in a separatory funnel with 10 mL of octanol for 2 min to remove any polar radiolabeled impurities accompanying the radiotracer. The aqueous phase was discarded, the octanol phase was retained, and four 2 mL aliquots of the octanol phase were pipetted into four test tubes each containing 2 mL of the phosphate buffer. The test tubes were capped and vigorously shaken for 10 min. After shaking, the test tubes were centrifuged at 300*g* for 5 min to thoroughly separate the two phases. For each of the four test tubes, a 0.5 mL portion of the upper octanol phase was pipetted into a tube for counting. The remainder of the octanol phase was carefully removed, the pipet tip was changed, and a 0.5 mL portion of the buffer phase was pipetted into a tube for counting. The radioactivity in the octanol and the phosphate buffers for each replicate were determined with a Packard Cobra II auto-gamma counter (Perkin-Elmer, Downers Grove, IL) and decay corrected. The log $P_{7.4}$ values were calculated for each replicate with the following equation:

$$\log P_{7.4} = \log [\text{counts in octanol phase/counts in buffer phase}]$$

The log $P_{7.4}$ measurements from each replication were averaged to give the log $P_{7.4}$ value for the radiotracer.

Rodent Biodistribution Studies. Tissue distribution studies were performed in male Sprague−Dawley rats (200−250 g) after intravenous injection of [^{123}I]ZIET in 0.1 to 0.4 mL of 10% ethanol/saline. The animals were allowed food and water ad libitum before the experiments. The animals were anesthetized with an intramuscular injection of 0.1 mL/100 g of a 1/1 ketamine (500 mg/mL)/xylazine (20 mg/mL) solution, and cannulas were placed in the tail veins. The animals were killed at the appropriate time points, their tissues were dissected, and selected tissues were weighed and counted along with dose standards in a Packard Cobra II auto-gamma counter. The raw counts were decay-corrected to a standard time, and the counts were normalized as the percent of total injected dose per gram of tissue (%ID/g). The statistical analyses of the rodent biodistribution studies were performed with GraphPad Prism software package for one-way analysis of variances (ANOVAs) and with SigmaStat software package (SPSS, Inc., Chicago, IL) for two-way ANOVAs. The reported *p*-values were calculated using Tukey's posthoc test for all pairwise comparisons.

Tissue distribution studies were performed in male Sprague−Dawley rats (200−250 g) after intravenous injection of ~20 μCi of [^{123}I]ZIET in 0.2 mL of 10% ethanol/saline. The rats were killed in groups of five at 5, 30, 60, and 120 min after injection of [^{123}I]ZIET. The brains of the rats were dissected, and the amount of radioactivity in the various brain regions was measured. In the blocking experiments, the rats were divided into four groups, and three of the groups were given a competing monoamine transporter ligand 15 min prior to the injection of [^{123}I]ZIET. The monoamine transporter ligands used in this study were RTI-113, reboxetine, and citalopram at doses of 4 mg/kg for each drug. The rats in each of the four groups were killed 60 min after the injection of [^{123}I]ZIET.

In Vitro Competition Assays. Competition assays were performed based on methods reported previously.[44,45] Cell membranes from human embryonic kidney cell line (HEK-293) stably expressing hNET or hSERT (gift from Dr. Randy Blakely, Vanderbilt University) and dog kidney cell line (MDCK) stably expressing hDAT (gift from Dr. Gary Rudnick, Yale University) were used in these assays. Cells were grown

to confluency in DMEM containing 10% fetal bovine serum and geneticin sulfate and then harvested using pH 7.4 phosphate-buffered saline (PBS) containing 0.53 mM ethylenediaminetetraacetic acid (EDTA) at 37 °C. Cell pellets were prepared through centrifugation at 2000*g* for 10 min, the supernatant was decanted, and the pellets were homogenized with a Polytron PT3000 (Brinkman, Littau, Switzerland) at 11 000 rpm for 12 s in 30 volumes of PBS. The resulting cell membrane suspensions were centrifuged at 43 000 × g for 10 min, the supernatants were decanted, and the resulting pellets were stored at −70 °C until used in assays. Competition assays were performed in 13 × 100 mm polystyrene tubes in a 2.0 mL final volume consisting of 1.7 mL of assay buffer, 100 μL of competing ligand in assay buffer, 100 μL of radioligand in assay buffer, and 100 μL of cell membrane suspension in assay buffer. Cell membrane pellets were characterized prior to competition assays to determine membrane concentrations that gave optimal signal while not significantly affecting the concentration of free radioligand. The cell membrane pellets were resuspended in the appropriate volume of assay buffer through brief homogenization using a Polytron PT3000 just prior to their use in assays. Competing ligands were assayed in triplicate at twelve concentrations ranging from 10^{-13} to 10^{-5} M. To ensure solubility, the competing ligands were dissolved in 1/1 ethanol/5 mM aqueous hydrochloric acid and then serially diluted in 5 mM hydrochloric acid. For SERT assays, the assay buffer consisted of 53 mM Tris buffer, 126 mM sodium chloride, and 5.3 mM potassium chloride (pH 7.9 at room temperature). The equilibrium incubation time was 2 h at room temperature. The radioligand used for SERT assays was [^{3}H]citalopram obtained from Dupont NEN (Boston, MA; 3100 GBq/mmol), and the measured K_d used for K_i calculation was 1.8 nM. For NET assays, the assay buffer consisted of 53 mM Tris buffer, 320 mM sodium chloride, and 5.3 mM potassium chloride (pH 7.4 at 4 °C). The equilibrium incubation time was 4 h at 4 °C. The radioligand used for NET assays was [^{3}H]nisoxetine obtained from Dupont NEN (3000 GBq/mmol), and the measured K_d used for K_i calculation was 0.71 nM. For DAT assays, the assay buffer consisted of 42 mM sodium phosphate buffer and 320 mM sucrose (pH 7.4 at room temperature). The equilibrium incubation time was 1 h at room temperature. The radioligand used for DAT assays was [^{123}I]RTI-55 obtained from DuPont NEN (81.4 TBq/mmol), and the measured K_d used for K_i calculation was 0.43 nM. The radioligand concentrations used in the assays were approximately 0.3 to 0.4 nM for both [^{3}H]citalopram and [^{3}H]-nisoxetine and 0.01 to 0.02 nM for [^{125}I]RTI-55. All assays were initiated by the addition of the cell membrane suspension. At the end of the incubation, the assays were terminated by the addition of ∼5 mL of assay buffer at 4 °C followed by rapid vacuum filtration with 3 × 5 mL washes with assay buffer at 4 °C through GF/B filters (Whatman, Inc., Clifton, NJ) presoaked in assay buffer containing 6 g of polyethylenimine per liter. In the case of [^{3}H]nisoxetine and [^{3}H]citalopram, the dried filters were placed in scintillation vials with 6 mL of liquid scintillation cocktail (Ultima Gold, Packard Bioscience, Merden, CT) and shaken. In the case of [^{125}I]RTI-55, the dried filters were placed in 12 × 60 mm glass test tubes and counted directly. The amount of radioactivity present on the filters was determined with a liquid scintillation counter (LKB 1209 Rackbeta, Perkin-Elmer Wallac, Inc., Gaithersburg, MD) in the case of the tritiated ligands or in a gamma-counter (LKB−Wallac RiaGamma 1274, Perkin-Elmer Wallac, Inc.) in the case of [^{125}I]RTI-55. The data from the competition curves were analyzed and K_i values calculated using GraphPad Prism software (GraphPad Software, San Diego CA). The K_i values were reported as the geometric mean of at least three separate assays for each compound unless otherwise stated.

Nonhuman Primate Imaging. MicroPET studies were performed using adult male rhesus and cynomologus monkeys (6−10 kg). The animals were fasted for 12 h prior to the PET studies. The animals were initially anesthetized with an intramuscular injection of Telazol (3 mg/kg), intubated, and then maintained on a 1% isoflurane/5% oxygen gas mixture throughout the imaging session. Respiration was maintained through a mechanical ventilator with measurement of expiratory oxygen and carbon dioxide levels to ensure physiological levels of respiration. The radiolabeled compounds were injected via the antecubital vein over the course of 5 min. Quantitative brain imaging studies employing [^{11}C]ZIET and [^{11}C]ZBrET were performed using a Concorde MicroPET P4 system (Knoxville, TN). In each study, the animal was positioned in the scanner with its head immobilized with a thermoplastic face mask (Tru Scan, Annapolis, MD). A transmission scan was obtained with a germanium-68 source prior to the PET study for attenuation correction of the emission data. Emission data acquired were subject to iterative reconstruction (OSEM, two iterations, 40 subsets) with no pre- or postfiltering to provide images with an isotropic resolution of 3 mm fwhm. For generation of time−activity curves, regions of interest (ROIs) were drawn manually based on the anatomical landmarks visible in reconstructed PET images using ASIPro software (Concorde, Knoxville, TN). Several imaging studies were performed using [^{11}C]ZIET and [^{11}C]ZBrET in rhesus and cynomologus monkeys with and without injection of pharmacological doses of monoamine transporter ligands. Emission data were collected in the MicroPET imaging studies continuously for 85 or 115 min after injection of [^{11}C]tropane and then binned for analysis.

Metabolite Analysis in Monkeys. Arterial plasma analyses of [^{11}C]ZIET and [^{11}C]ZBrET metabolism were performed in rhesus and cynomolgus monkeys, respectively. [^{11}C]tropanes were injected as described above and arterial blood samples (4 mL) were collected at approximately 5, 40, 60, 80 min after tracer injection. The blood was centrifuged and the plasma separated. Acetonitrile (0.7 mL) was added to 0.5 mL of plasma sample, and the resulting suspension was vortexed then centrifuged at 10000 rpm for 3 min. The supernatant was removed and filtered through a 0.45 μm PTFE membrane. A 0.5 mL amount of the filtrate was injected and analyzed by HPLC with a UV detector (254 nm) and a flow-through radioactivity detector. Chromatographic separation was performed with a Waters, X-terra RP_{18} column (3.5 × 8 mm), a mobile phase of methanol:water:triethylamine 80:20:0.1, and a flow rate of 1.5 mL/min. Low activity samples (i.e. 40, 60, and 80 min) were also fractionated (0.5 min collections) and measured for radioactivity using a Packard Cobra automatic gamma-counter. All activity measurements were half-life decay-corrected.

Acknowledgment. This research was sponsored by the Office of Health and Environmental Research, U.S. Department of Energy under Grant No. DE-FG02-97ER62637 and the Emory Conte Center for the Neuroscience of Mental Disorders.The authors would like to thank Mary David for assistance in preparation of this manuscript. We also acknowledge the use of Shared Instrumentation provided by grants from the NIH and NSF.

References

(1) Fujita, M.; Shimada, S.; Maeno, H.; Nishimura, T.; Tohyama, M. Cellular localization of serotonin transporter mRNA in the rat brain. *Neurosci. Lett.* **1993**, *162*, 59−62.
(2) Austin, M. C.; Bradley, C. C.; Mann, J. J.; Blakely, R. D. Expression of serotonin transporter messenger RNA in the human brain. *J. Neurochem.* **1994**, *62*, 2362−2367.
(3) Hansson, S. R.; Mezey, E.; Hoffman, B. J. Serotonin transporter messenger RNA in the developing rat brain: early expression in serotonergic neurons and transient expression in non- serotonergic neurons. *Neuroscience* **1998**, *83*, 1185−1201.
(4) Pickel, V. M.; Chan, J. Ultrastructural localization of the serotonin transporter in limbic and motor compartments of the nucleus accumbens. *J. Neurosci.* **1999**, *19*, 7356−7366.
(5) Stockmeier, C. A.; Shapiro, L. A.; Haycock, J. W.; Thompson, P. A.; Lowy, M. T. Quantitative subregional distribution of serotonin$_{1A}$ receptors and serotonin transporters in the human dorsal raphe. *Brain Res.* **1996**, *727*, 1−12.
(6) Laakso, A.; Hietala, J. PET studies of brain monoamine transporters. *Curr. Pharm. Des.* **2000**, *6*, 1611−1623.

(7) Gurevich, E. V.; Joyce, J. N. Comparison of [^{3}H]paroxetine and [^{3}H]cyanoimipramine for quantitative measurement of serotonin transporter sites in human brain. *Neuropsychopharmacology* **1996**, *14*, 309−323.
(8) Owens, M. J.; Nemeroff, C. B. The Serotonin Transporter and Depression. *Depression Anxiety* **1998**, *8* (Suppl. 1), 5−6.
(9) Palmer, A. M.; Francis, P. T.; Benton, J. S.; et al. Presynaptic Serotonergic Dysfunction in Patients with Alzheimer's Disease. *J. Neurochem.* **1987**, *48*, 8−15.
(10) Cash, R.; Raisman, R.; Ploska, A. Y. High and Low Affinity [^{3}H]-Imipramine Binding Sites in Control and Parkinsonian Brain. *Eur. J. Pharmacol.* **1985**, *117*, 71−80.
(11) Chingaglia, G.; Landwehrmeyer, B.; Probst, A.; Palacios, J. M. Serotonergic Terminal Transporters are Differentially Affected in Parkinson's Disease and Progressive Supranuclear Palsy: An Autoradiographic Study with [^{3}H]Citalopram. *Neuroscience* **1993**, *54*, 691−699.
(12) Squier, M. V.; Jalloh, S.; Hilton-Jones, D.; Series, H. Death After Ectasy Ingestion: Neuropathological Findings. *J. Neurol., Neurosurg. Psychiatry* **1995**, *58*, 756.
(13) Halldin, C.; Gulyas, B.; Langer, O.; Farde, L. Brain radioligands-state of the art and new trends. *Q. J. Nucl. Med.* **2001**, *45*, 139−152.
(14) Laruelle, M.; Slifstein, M.; Huang, Y. Positron emission tomography: imaging and quantification of neurotransporter availability. *Methods* **2002**, *27*, 287−299.
(15) Huang, Y.; Hwang, D. R.; Narendran, R.; Sudo, Y.; Chatterjee, R.; Bae, S. A.; Mawlawi, O.; Kegeles, L. S.; Wilson, A. A.; Kung, H. F.; Laruelle, M. Comparative evaluation in nonhuman primates of five PET radiotracers for imaging the serotonin transporters: [^{11}C]McN 5652, [^{11}C]ADAM, [^{11}C]DASB, [^{11}C]-DAPA, and [^{11}C]AFM. *J. Cereb. Blood Flow Metab.* **2002**, *22*, 1377−1398 and references cited.
(16) Kuikka, J. T.; Tiihonen, J.; Bergstrom, K. A.; Karhu, J.; Hartikainen, P.; Viinamaki, H.; Lansimies, E.; Lehtonen, J.; Hakola, P. Imaging of serotonin and dopamine transporters in the living human brain. *Eur. J. Nucl. Med.* **1995**, *22*, 346−350.
(17) Maryanoff, B. E.; McComsey, D. F.; Gardocki, J. F.; Shank, R. P.; Costanzo, M. J.; Nortey, S. O.; Schneider, C. R.; Setler, P. E. Pyrroloisoquinoline antidepressants. 2. In-depth exploration of structure−activity relationships. *J. Med. Chem.* **1987**, *30*, 1433−1454.
(18) Suehiro, M.; Scheffel, U.; Dannals, R. F.; Ravert, H. T.; Ricaurte, G. A.; Wagner, H. N., Jr. A PET radiotracer for studying serotonin uptake sites: carbon-11-McN-5652Z. *J. Nucl. Med.* **1993**, *34*, 120−127.
(19) Suehiro, M.; Scheffel, U.; Ravert, H. T.; Dannals, R. F.; Wagner, H. N., Jr. [^{11}C](+)McN5652 as a radiotracer for imaging serotonin uptake sites with PET. *Life Sci.* **1993**, *53*, 883−892.
(20) Acton, P. D.; Choi, S. R.; Hou, C.; Plossl, K.; Kung, H. F. Quantification of serotonin transporters in nonhuman primates using [^{123}I]ADAM and SPECT. *J. Nucl. Med.* **2001**, *42*, 1556−1562.
(21) Houle, S.; Ginovart, N.; Hussey, D.; Meyer, J. H.; Wilson, A. A. Imaging the serotonin transporter with positron emission tomography: initial human studies with [^{11}C]DAPP and [^{11}C]-DASB. *Eur. J. Nucl. Med.* **2000**, *27*, 1719−1722.
(22) Wilson, A. A.; Ginovart, N.; Hussey, D.; Meyer, J.; Houle, S. In vitro and in vivo characterisation of [^{11}C]-DASB: a probe for in vivo measurements of the serotonin transporter by positron emission tomography. *Nucl. Med. Biol.* **2002**, *29*, 509−515.
(23) Huang, Y.; Bae, S. A.; Zhu, Z.; Guo, N.; Hwang, D. R.; Laruelle, M. Fluorinated Analogues of ADAM as New PET Radioligands for the Serotonin Transporter: Synthesis and Pharmacologic Evaluation. *J. Labelled Compd. Radiopharm.* **2001**, *44* (suppl. 1), S18−20.
(24) Jarkas, N.; McConathy, J.; Ely, T.; Kilts, C. D.; Votaw, J. R.; Goodman, M. M. Synthesis and radiolabeling of new derivatives of ADAM. *J. Labelled Compd. Radiopharm.* **2001**, *44*, S204−206.
(25) Oya, S.; Choi, S. R.; Coenen, H.; Kung, H. F. New PET Imaging Agent for the Serotonin Transporter: [^{18}F]ACF (2-[(2-Amino-4-chloro-5-fluorophenyl)thio]-*N*,*N*-dimethyl-benzenmethanamine). *J. Med. Chem.* **2002**, *45*, 4716−4723.
(26) Blough, B. E.; Abraham, P.; Lewin, A. H.; Kuhar, M. J.; Boja, J. W.; Carroll, F. I. Synthesis and transporter binding properties of 3 beta-(4′-alkyl-, 4′- alkenyl-, and 4′-alkynylphenyl)nortropane-2 beta-carboxylic acid methyl esters: serotonin transporter selective analogues. *J. Med. Chem.* **1996**, *39*, 4027−4035.
(27) Blough, B. E.; Abraham, P.; Mills, A. C.; Lewin, A. H.; Boja, J. W.; Scheffel, U.; Kuhar, M. J.; Carroll, F. I. 3 Beta-(4-ethyl-3-iodophenyl)nortropane-2 beta-carboxylic acid methyl ester as a high-affinity selective ligand for the serotonin transporter. *J. Med. Chem.* **1997**, *40*, 3861−3864.
(28) Goodman, M. M.; Chen, P.; Plisson, C.; Martarello, L.; Galt, J.; Votaw, J. R.; Kilts, C. D.; Malveaux, E. J.; Camp, V. M.; Shi, B.; Ely, T. D.; Howell, L.; McConathy, J.; Nemeroff, C. B.; Synthesis and Characterization of Iodine-123 Labeled 2−Carbomethoxy-3-(4′-((*Z*)-2-iodoethenyl)phenyl)nortropane. A Ligand for In Vivo Imaging of Serotonin Transporters by Single Photon Emission Tomography. *J. Med. Chem.* **2003**, *46*, 925−935.
(29) Carroll, F. I.; Gao, Y.; Abdur Rahman, M.; Abraham, P.; Parham, K.; Lewin, A. H.; Boja, J. W.; Kuhar, M. J. Synthesis, Ligand Binding, QSAR, and CoMFA Study of 3β-(*p*-Substitutedphenyl)-tropane-2β-carboxylic Acid Methyl Esters. *J. Med. Chem.* **1991**, *34*, 2719−2725.
(30) Goodman, M. M.; Chen, P.; Kilts, C. D.; Ely, T.; Davis, M.; Votaw, J. Fluorine-18 Serotonin Transporter Ligands. *Synthesis and Applications of Isotopically Labelled Compounds* **2001**, *7*, 362−365.
(31) Meegalla, S. K.; Plössl, K.; Kung, M.-P.; Mu, M.; Kung, H. F. Stuctureactivity Relationship of [^{99m}Tc]TRODAT-1 Derivatives as New Dopamine Transporter Imaging Agents. *J. Labelled Cpd. Radiopharm.* **1997**, *40*, 434−436.
(32) Mitchell, T. N.; Amaria, A.; Killing, H.; Rutshow, D. Palladium Catalysis in Organotin Chemistry: Addition of Hexaalkylditins to Alkynes. *J. Organomet. Chem.* **1986**, *304*, 257−265.
(33) Blough, B. E.; Keverline, Z. N.; Navarro, H.; Kuhar, M. J.; Carroll F. I. Synthesis and Transporter Binding Properties of 3β-[4′-(Phenylalkyl, -phenylalkenyl, and -phenylalkynl)phenyl]tropane-2β-carboxylic Acid Methyl Esters: Evidence of a Remote Phenyl Binding Domain on the Dopamine Transporter. *J. Med. Chem.* **2002**, *45*, 4029−4037.
(34) Uenishi, J.; Kawahama, R.; Yonemitsu, O. Stereoselective Hydrogenolysis of 1,1-Dibromo-1-alkenes and Stereospecific Synthesis of Conjugated (*Z*)-Alkenyl Compounds. *J. Org. Chem.* **1998**, *63*, 8965−8975.
(35) Boja, J. W.; Kuhar, M. J.; Kopajtic, T.; Yang, E.; Abraham, P.; Lewin, A. H.; Carroll, F. I. Secondary amine analogues of 3 beta-(4′-substituted phenyl)tropane-2 beta-carboxylic acid esters and *N*-norcocaine exhibit enhanced affinity for serotonin and norepinephrine transporters. *J. Med. Chem.* **1994**, *37*, 1220−1223.
(36) Carroll, F. I.; Kotian, P.; Dehghani, A.; Gray, J. L.; Kazembo, M. A.; Parham, K. A.; Abraham, P.; Lewin, A. H.; Boja, J. W.; Kuhar, M. J. Cocaine and 3β-(4′-Substituted phenyl)tropane-2β-carboxylic Acid Ester and Amide Analogues. New High-Affinity and Selective Compounds for the Dopamine Transporter. *J. Med. Chem.* **1995**, *38*, 379−388.
(37) Owens, M. J.; Knight, D. L.; Nemeroff, C. B. Second-Generation SSRIs: Human Monoamine Transporter Binding Profile of Escitalopram and *R*-Fluoxetine. *Biol. Psychiatry* **2001**, *50*, 345−350.
(38) Wong, E. H. F.; Sonders, M. S.; Amara, S. G.; Tinholt, P. M.; Piercey, M. F. P.; Hoffman, W. P.; Hyslop, D. K.; Franklin, S.; Porsolt, R. D.; Bonsignori, A.; Carfagna, N.; McArthur, R. A. Reboxetine: A Pharmacologically Potent, Selective, and Specific Norepinephrine Reuptake Inhibitor. *Biol. Psychiatry* **2000**, *47*, 818−829.
(39) Jarkas, N.; McConathy, J.; Malveaux, G.; Camp, M.; Williams, L.; Votaw, J.; Kilts, C. D.; Goodman, M. M. Synthesis and Pharmacological Characterization of Carbon-11 *N*,*N*-dimethyl-2-(2′-amino-4′-hydroxymethylphenylthio)benzylamine (HOMADAM): an Improved Serotonin Transporter Imaging Agent. *J. Nucl. Med.* in preparation.
(40) Wilson, A. A.; Houle, J. N. Radiosynthesis of Carbon-11 labeled *N*-Methyl-2-(arylthio)benzylamines: Potential Radiotracers for the Serotonin Reuptake Receptor. *J. Labelled Compd. Radiopharm.* **1999**, *42*, 1277−1288.
(41) Kessler, R. M.; Ansari, M. S.; dePaulis, T.; Schimdt, D. E.; Clanton, J. A.; Smith, H. E.; Manning, R. G.; Gillepsie, D.; Ebert, M. H. High affinity dopamine receptor D_2 radioligands 1. Regional rat brain distribution of iodinated benzamides. *J. Nucl. Med.* **1991**, *32*, 1593−1600.
(42) Lundlvist, C.; Halldin, C.; Swahn, C.-G.; Ginovart, N.; Farde, L. Different Brain Radioactivity Curves in a PET Study with [^{11}C]β-CIT Labeled in Two Different Positions. *Nucl. Med. Biol.* **1999**, *26*, 343−350.
(43) Lemaire, C.; Plenevaux, A.; Aerts, J.; Del Fiore, G.; Brihaye, C.; Le Bars, D.; Comar, D.; Luxen, A. Solid-Phase Extraction − An Alternative to the Use of Rotary Evaporators for Solvent Removal in the Rapid Formulation of PET Radiopharmaceuticals. *J. Labelled Compd. Radiopharm.* **1999**, *42*, 63−75.
(44) Owens, M. J.; Morgan, W. N.; Plott, S. J.; Nemeroff, C. B. Neurotransmitter receptor and transporter binding profile of antidepressants and their metabolites. *J. Pharmacol. Exp. Ther.* **1997**, *283*, 1305−1322.
(45) Goodman, M. M.; Kilts, C. D.; Keil, R.; Shi, B.; Martarello, L.; Xing, D.; Votaw, J.; Ely, T. D.; Lambert, P.; Owens, M. J.; Camp, V. M.; Malveaux, E.; Hoffman, J. M. ^{18}F-labeled FECNT: a selective radioligand for PET imaging of brain dopamine transporters. *Nucl. Med. Biol.* **2000**, *27*, 1−12.

JM030384E